Electronic Supplementary Material (ESI) for Chemical Science.

Supplementary Information

One-Pot Cascade Construction of Nonsubstituted Quinoline-Bridged Covalent Organic Frameworks

Huaji Pang[1], Dekang Huang[1], Yanqiu Zhu[1], Xiaodong Zhao[1] & Yonggang Xiang[1*]

[1]Department of Chemistry, College of Science, Huazhong Agricultural University, Wuhan, Hubei 430070, China

E-mail: ygxiang@mail.hzau.edu.cn

Table of Contents

1. General information

1.1 Reagents

Unless otherwise noted, all the chemicals and reagents were purchased in analytical purity from commercial suppliers and used directly without further purification. Karl Fischer reagent (containing pyridine) was purchased from Sinopharm Chemical Reagent Co., Ltd., 4,4',4",4"'-(pyrene-1,3,6,8-tetrayl)tetrabenzaldehyde (**D**), 4,4',4",4"'-(pyrene-1,3,6,8-tetrayl)tetrakis(2-methoxybenzaldehyde) (**E**), and 4,4',4",4"'-(pyrene-1,3,6,8-tetrayl)tetraaniline (**3**) were synthesized following the reported procedures.[1]

1.2 Characterization methods

Powder X-ray diffraction (PXRD) patterns were collected on a Bruker D8 Advance diffractometer with Cu Kα radiation (2θ range: 2-40°; Scan step size: 0.02°; Time per step: 1 s). Liquid-state ^{1}H NMR, ^{13}C NMR, and ^{19}F NMR were recorded on Bruker Advance 600 MHz, 150 MHz, and 564 MHz spectrometers at 298 K, respectively, and chemical shift (δ) was reported in ppm with residual solvent peak as the reference. Peaks are reported as follows: s = singlet, d = doublet, t = triplet, q = quartet, m = multiplet or unresolved, with coupling constants in Hz. Fourier transform infrared (FT-IR) spectra were collected on a Nicolet 6700 spectrometer (Thermo Scientific, USA) equipped with an ATR cell. The specific Brunauer-Emmett-Teller (BET) surface area and pore size distribution were measured using a Micrometrics ASAP 2040 instrument at 77 K. High resolution transmission electron microscope (HRTEM) images were obtained on a JEM-2100F instrument at an accelerating voltage

of 200 kV. Solid-state ^{13}C cross polarization magic angle spinning (^{13}C-CP/MAS) NMR spectra were collected on a Bruker Avance III HD 400 spectrometer. X-ray photoelectron spectroscopy (XPS) measurements were performed on a Thermo ESCALAB 250 spectrometer with non-monochromatic Al Kα x-rays as the excitation source and C 1s (284.8 eV) as the reference line. Solid-state diffuse reflectance Ultraviolet–visible spectroscopy (UV-vis) spectra were collected on a Shimadzu UV 3600 Spectrophotometer with $BaSO_4$ as the reference. Thermal stability was investigated on a DSC 200 PC (NETZSCH) thermogravimetric analyzer with temperature ranging from 303 to 1073 K under N_2 atmosphere at a heating rate of 5 K min^{-1}. The generation of $O_2^{\bullet-}$ was determined by electron paramagnetic resonance (EPR) spectra, which was recorded on a JES-FA200 spectrometer under visible light irradiation using 5,5-dimethyl-1-pyrroline-N-oxide (DMPO) as the spin trapper.

1.3 Electrochemical measurements

Electrochemical measurements were performed on the CHI660E workstation (Chenhua Instruments, China), and the standard three-electrode system included a platinum plate as the counter electrode, a commercial Ag/AgCl electrode as the reference electrode, and a working electrode. The working electrode was prepared as follows: 15 mg of sample was thoroughly mixed with 200 μL isopropanol containing 5% Nafion, and the resulting suspension was carefully loaded on the ITO glass substrate (10 × 25 × 1.1 mm) and dried at 60 ºC under vacuum for 1 h. 0.1 M Na_2SO_4 aqueous solution was employed as the electrolyte for the photocurrent test while the aqueous solution containing 0.1 M KCl and 0.005 M $K_3[Fe(CN)_6]$ was employed as the

electrolyte for the electrochemical impedance spectroscopy (EIS) measurement. For Mott-Schottky tests, the perturbation was 5 mV with frequencies of 100, 500, and 1000 Hz.

2. Synthesis of small molecules

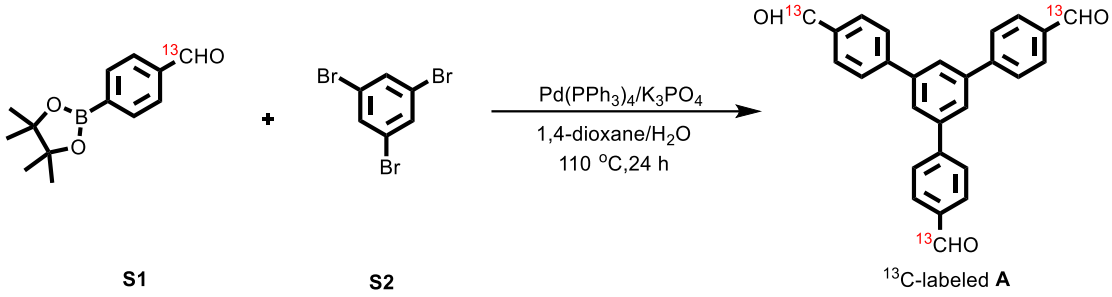

S1 **S2** ^{13}C-labeled **A**

^{13}C-labeled A: A round-bottom flask was charged with ^{13}C-labeled **S1**[1] (464 mg, 2 mmol), 1,3,5-tribromobenzene (157 mg, 0.5 mmol), $Pd(PPh_3)_4$ (28.89 mg, 0.025 mmol) and K_3PO_4 (0.743 g, 3.5 mmol), and a mixed solvent of 1,4-dioxane (15 mL), distilled water (2 mL). After being degassed with Ar for 10 min, the mixture was stirred at 110 °C under an Ar atmosphere for 24 h. After cooling down, water was added to quench the reaction, and the mixture was extracted with ethyl acetate (EA) three times. The combined organic phases were washed with brine and dried over anhydrous Na_2SO_4. The concentrated residue was purified by flash chromatography on silica gel with CH_2Cl_2 as the eluent to afford the product ^{13}C-labeled **A** as a white solid (180 mg, 93%). ^{1}H NMR (600 MHz, $CDCl_3$) δ 10.25-9.96 (dd, 3H), 8.03-8.01 (m, 6H), 7.91 (s, 3H), 7.88 (d, J = 8.2 Hz, 6H); ^{13}C NMR (151 MHz, $CDCl_3$) δ 191.9, 146.4, 141.7, 136.0, 130.6, 128.1, 126.6.

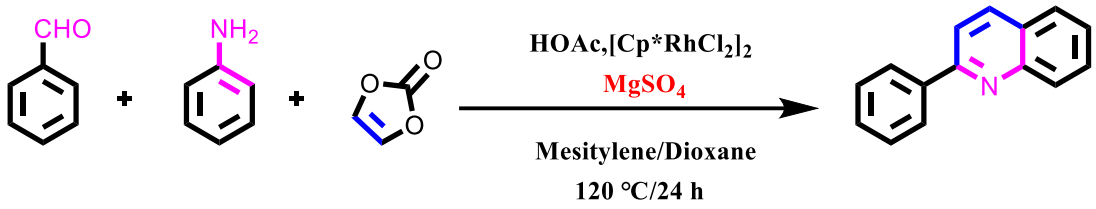

Model reaction for the synthesis of 2-phenylquinoline: A 10 mL Schlenk pressure tube was charged with benzaldehyde (31.8 mg, 0.30 mmol), aniline (27.9 mg, 0.30 mmol), vinylene carbonate (51.6 mg, 0.60 mmol), $[Cp^*RhCl_2]_2$ (4 mg, 0.003 mmol), and mesitylene (1 mL) and dioxane (1 mL). After being sonicated for 5 minutes, the tube was degassed by three freeze-pump-thaw cycles (liquid nitrogen) and sealed under vacuum. Subsequently, the reaction mixture was stirred at 120 °C for 24 h. After cooling down, the concentrated residue was purified by flash chromatography on silica gel with PE/EA as the eluent to afford the product **2-phenylquinoline** (58.5 mg, 0.28 mmol, 95%). ^{1}H NMR ($CDCl_3$, 600 MHz) δ 8.25-8.17 (m, 4H), 7.89 (d, J = 7.9 Hz, 1H), 7.85 (d, J = 7.9 Hz, 1H), 7.75 (t, J = 7.5 Hz, 1H), 7.55-7.52 (m, 3H), 7.48 (t, J = 7.5 Hz, 1H); ^{13}C NMR (151 MHz, $CDCl_3$) δ 157.3, 148.2, 139.6, 136.7, 129.7, 129.6, 129.3, 128.8, 127.5, 127.4, 127.1, 126.2, 118.9.

3. One-pot synthesis of NQ-COFs

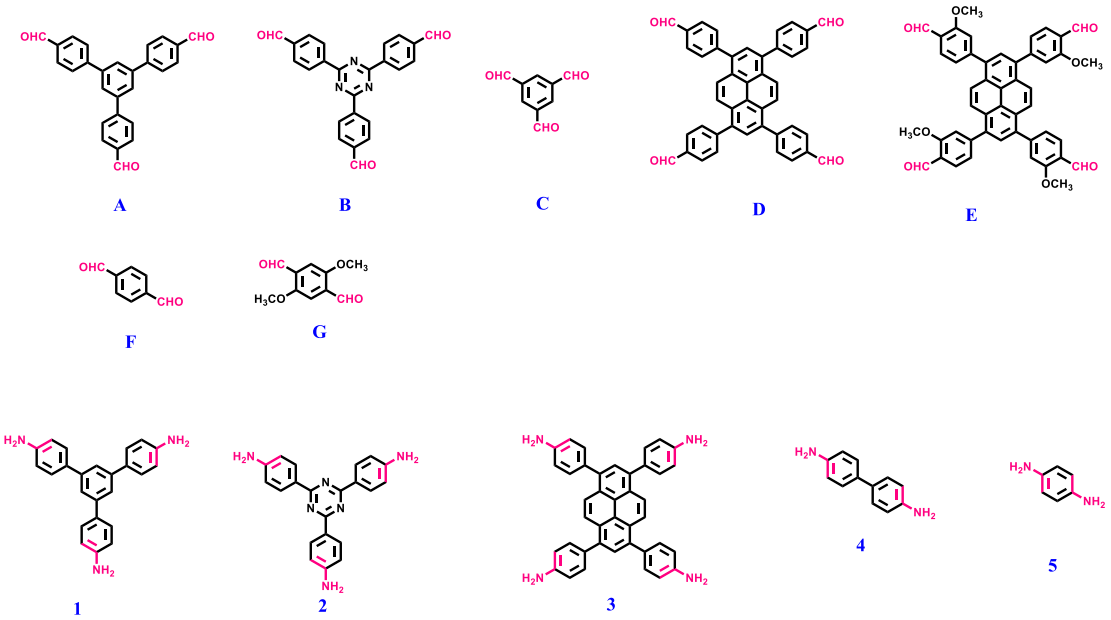

Supplementary Scheme 1. Chemical structures of the building blocks for synthesis of NQ-COFs

Supplementary Table 1. Condition optimization for the synthesis of **NQ-COF$_{A1}$-OPR**.[a]

Entry	Solvent	Catalyst	$MgSO_4$ (mg)	Crystallinity
1	*o*-DCB 1 mL	HOAc 50μL	72	Low
2	*o*-DCB 1 mL	HOAc 50μL	-	No
3	*o*-DCB 1 mL	6 M HOAc 100 μL	72	No
4	*o*-DCB 1 mL	6 M HOAc 100 μL	-	No
5	*o*-DCB 1 mL	TFA 50 μL	72	Low
6	*o*-DCB 1 mL	TFA 50 μL	-	No
7	Dioxane 1mL	HOAc 50 μL	72	No
8	Dioxane 1mL	HOAc 50 μL	-	No
9	Dioxane 1mL	6 M HOAc 100 μL	72	No
10	Dioxane 1mL	6 M HOAc 100 μL	-	No
11	Dioxane 1mL	TFA 50 μL	72	No
12	Dioxane 1mL	TFA 50 μL	-	No
13	Mesitylene: Dioxane=1:1	HOAc 50 μL	72	Moderate
14	Mesitylene: Dioxane=1:1	HOAc 50 μL	-	No
15	Mesitylene: Dioxane=1:1	6 M HOAc 100 μL	72	No
16	Mesitylene: Dioxane=1:1	6 M HOAc 100 μL	-	No
17	Mesitylene: Dioxane=1:1	TFA 50 μL	72	Low
18	Mesitylene: Dioxane=1:1	TFA 50 μL	-	No
19	Mesitylene: Dioxane=1:2	HOAc 50 μL	72	High
10	Mesitylene: Dioxane=1:2	HOAc 50 μL	-	No
21	Mesitylene: Dioxane=1:2	6 M HOAc 100 μL	72	No
22	Mesitylene: Dioxane=1:2	6 M HOAc 100 μL	-	No
23	Mesitylene: Dioxane=1:2	TFA50 μL	72	No
24	Mesitylene: Dioxane=1:2	TFA50 μL	-	No
25	Mesitylene: Dioxane=2:1	HOAc 50 μL	72	Low
26	Mesitylene: Dioxane=2:1	HOAc 50 μL	-	No
27	Mesitylene: Dioxane=2:1	6 M HOAc 100 μL	72	Low
28	Mesitylene: Dioxane=2:1	6 M HOAc 100 μL	-	No
29	Mesitylene: Dioxane=2:1	TFA50 μL	72	No
30	Mesitylene: Dioxane=2:1	TFA50 μL	-	No
31	*o*-DCB: *n*-BuOH =1:1	HOAc 50 μL	72	Low
32	*o*-DCB: *n*-BuOH =1:1	HOAc 50 μL	-	No
33	*o*-DCB: *n*-BuOH =1:1	6 M HOAc 100 μL	72	No
34	*o*-DCB: *n*-BuOH =1:1	6 M HOAc 100 μL	-	No
35	*o*-DCB: *n*-BuOH =1:1	TFA50 μL	72	Low
36	*o*-DCB: *n*-BuOH =1:1	TFA50 μL	-	No
37	*o*-DCB: *n*-BuOH =1:2	HOAc 50 μL	72	Moderate
38	*o*-DCB: *n*-BuOH =1:2	HOAc 50 μL	-	No

39	*o*-DCB: *n*-BuOH =1:2	6 M HOAc 100 μL	72	Low
40	*o*-DCB: *n*-BuOH =1:2	6 M HOAc 100 μL	-	No
41	*o*-DCB: *n*-BuOH =1:2	TFA50 μL	72	No
42	*o*-DCB: *n*-BuOH =1:2	TFA50 μL	-	No
43	*o*-DCB: *n*-BuOH =2:1	HOAc 50 μL	72	Low
44	*o*-DCB: *n*-BuOH =2:1	HOAc 50 μL	-	No
45	*o*-DCB: *n*-BuOH =2:1	6 M HOAc 100 μL	72	Low
46	*o*-DCB: *n*-BuOH =2:1	6 M HOAc 100 μL	-	No
47	*o*-DCB: *n*-BuOH =2:1	TFA50 μL	72	Low
48	*o*-DCB: *n*-BuOH =2:1	TFA50 μL	-	No
49	*o*-DCB: *i*-PrOH =1:1	HOAc 50 μL	72	No
50	*o*-DCB: *i*-PrOH =1:1	HOAc 50 μL	-	No
51	*o*-DCB: *i*-PrOH =1:1	6 M HOAc 100 μL	72	No
52	*o*-DCB: *i*-PrOH =1:1	6 M HOAc 100 μL	-	No
53	*o*-DCB: *i*-PrOH =1:1	TFA50 μL	72	No
54	*o*-DCB: *i*-PrOH =1:1	TFA50 μL	-	No
55	DMAc: Mesitylene: Dioxane=2:2:1	HOAc 50 μL	72	Moderate
56	DMAc: Mesitylene: Dioxane=2:2:1	HOAc 50 μL	-	No
57	DMAc: Mesitylene: Dioxane=2:2:1	6 M HOAc 100 μL	72	Low
58	DMAc: Mesitylene: Dioxane=2:2:1	6 M HOAc 100 μL	-	No
59	DMAc: Mesitylene: Dioxane=2:2:1	TFA50 μL	72	Low
60	DMAc: Mesitylene: Dioxane=2:2:1	TFA50 μL	-	No
61	Mesitylene: Dioxane: *n*-BuOH=1:1:1	HOAc 50 μL	72	Low
62	Mesitylene: Dioxane: *n*-BuOH=1:1:1	HOAc 50 μL	-	No
63	Mesitylene: Dioxane: *n*-BuOH=1:1:1	6 M HOAc 100 μL	72	No
64	Mesitylene: Dioxane: *n*-BuOH=1:1:1	6 M HOAc 100 μL	-	No
65	Mesitylene: Dioxane: *n*-BuOH=1:1:1	TFA50 μL	72	Low
66	Mesitylene: Dioxane: *n*-BuOH=1:1:1	TFA50 μL	-	No

[a] Aldehyde A, amine 1, vinylene carbonate (3 equiv), 120 ℃, 3 d.

One-pot synthesis of 12 other NQ-COFs: The synthetic condition is similar to that of **NQ-COF$_{A1}$-OPR** with only the amount of building blocks, types of catalyst, and solvent changed, and the optimized reaction conditions were demonstrated in Supplementary Table 2.

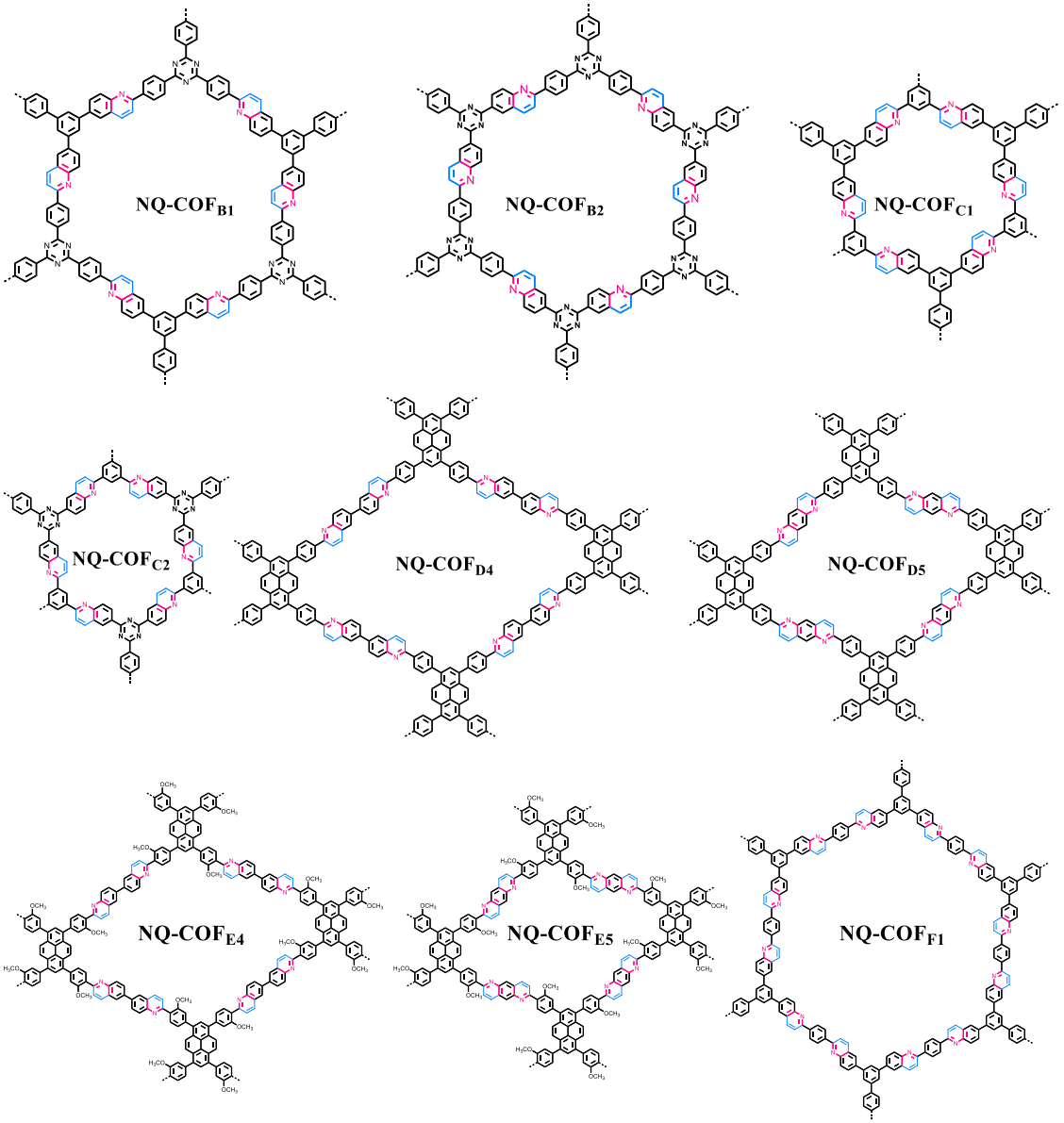

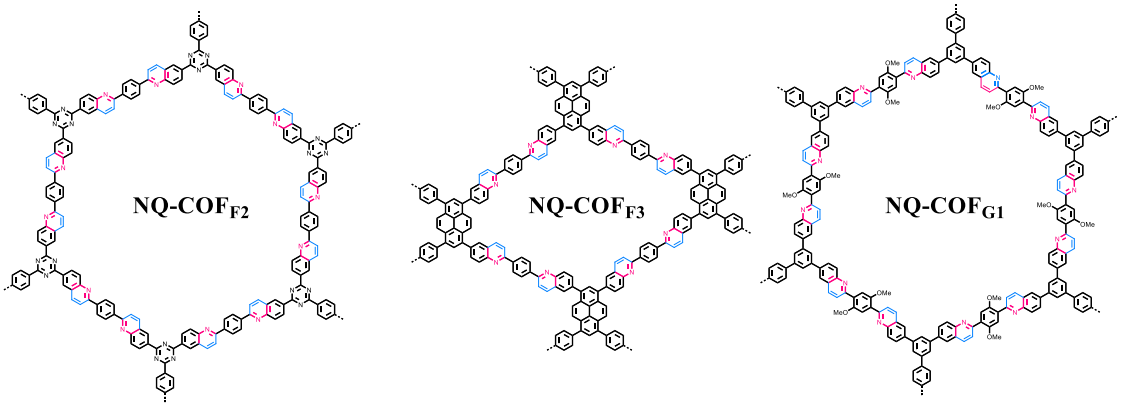

Supplementary Scheme 2. Chemical structures of different **NQ-COFs**.

Supplementary Table 2. Optimized reaction conditions for one-pot synthesis of different **NQ-COFs**.

Entry	Aldehyde	Amine	Acid	Solvent **1**	Solvent **2**	Solvent **3**	Yield
NQ-COF$_{B1}$	19.7 mg 0.05 mmol	17.6 mg 0.05 mmol	HOAc (0.05 mL)	Mesitylene (1.0 mL)	Dioxane (0.5 mL)	-	36.2 mg 95%
NQ-COF$_{B2}$	19.7 mg 0.05 mmol	17.7 mg 0.05 mmol	HOAc (0.05 mL)	*o*-DCB (0.5 mL)	*i*-PrOH (0.5 mL)	-	36.0 mg 94%
NQ-COF$_{C1}$	8.1 mg 0.05 mmol	17.6 mg 0.05 mmol	HOAc (0.05 mL)	*o*-DCB (0.5 mL)	*n*-BuOH (1.0 mL)	-	24.5 mg 92%
NQ-COF$_{C2}$	8.1 mg 0.05 mmol	17.7 mg 0.05 mmol	HOAc (0.05 mL)	*o*-DCB (0.5 mL)	*n*-BuOH (1.0 mL)	-	24.0 mg 90%
NQ-COF$_{D4}$	30.9 mg 0.05 mmol	18.4 mg 0.10 mmol	HOAc (0.05 mL)	*o*-DCB (1.0 mL)	-	-	46.6 mg 92%
NQ-COF$_{D5}$	30.9 mg 0.05 mmol	10.8 mg 0.10 mmol	TFA (0.05 mL)	*o*-DCB (1.0 mL)	-	-	39.5 mg 92%
NQ-COF$_{E4}$	36.9 mg 0.05 mmol	18.4 mg 0.10 mmol	TFA (0.05 mL)	*o*-DCB (1.0 mL)	-	-	49.2 mg 87%
NQ-COF$_{E5}$	36.9 mg 0.05 mmol	10.8 mg 0.10 mmol	TFA (0.05 mL)	*o*-DCB (1.0 mL)	-	-	43.5 mg 89%
NQ-COF$_{F1}$	10.6 mg 0.075 mmol	17.6 mg 0.05 mmol	TFA (0.05 mL)	Mesitylene (0.5 mL)	Dioxane (0.5 mL)	*n*-BuOH (0.5 mL)	25.9 mg 92%
NQ-COF$_{F2}$	10.6 mg 0.075 mmol	17.7 mg 0.05 mmol	HOAc (0.05 mL)	*o*-DCB (1.0 mL)	-	-	26.2 mg 93%
NQ-COF$_{F3}$	13.4 mg 0.10 mmol	28.3 mg 0.05 mmol	TFA (0.05 mL)	*o*-DCB (1.0 mL)	-	-	38.6 mg 90%
NQ-COF$_{G1}$	14.6 mg 0.075 mmol	17.6 mg 0.05 mmol	HOAc (0.05 mL)	*o*-DCB (1.0 mL)	-	-	30.3 mg 93%

4. Structure Modeling and PXRD Refinement of NQ-COFs

Supplementary Table 3. The Pawley refinement results including unit cell parameters and final related refinement factors for NQ-COFs

NQ-COF	Unit cell parameters	Space group	Refinement factors
NQ-COF$_{A1}$-OPR	a = 25.47 Å b = 26.22 Å c = 3.59 Å α = β = 90° γ = 120°	*P1*	Rwp = 1.49 % Rp = 1.11%
NQ-COF$_{B1}$	a = 25.87 Å b = 25.89 Å c = 3.53 Å α = β = 90° γ = 120°	*P1*	Rwp = 1.48 % Rp = 0.83 %
NQ-COF$_{B2}$	a = 25.16 Å b =26.27 Å c = 3.51 Å α = β = 90° γ = 120°	*P1*	Rwp = 1.66 % Rp = 1.45 %
NQ-COF$_{C1}$	a = 18.62 Å b = 18.61 Å c = 3.63 Å α = β = 90° γ = 120°	*P1*	Rwp = 2.38 % Rp = 1.53 %
NQ-COF$_{C2}$	a = 19.04 Å b = 17.79 Å c= 3.35 Å α = β = 90° γ = 120°	*P1*	Rwp = 1.30 % Rp = 1.21 %
NQ-COF$_{D4}$	a = 28.05 Å b = 28.52 Å c = 3.74 Å α = β = γ = 90°	*P1*	Rwp = 1.65 % Rp = 1.28 %

NQ-COF$_{D5}$	a = 23.93 Å b = 24.23 Å c = 3.75 Å α = β = γ = 90°	*P1*	Rwp = 1.32 % Rp = 1.19 %
NQ-COF$_{E4}$	a = 28.17 Å b = 28.65 Å c = 3.81 Å α = β = γ = 90°	*P1*	Rwp = 1.27 % Rp = 1.19 %
NQ-COF$_{E5}$	a = 23.85 Å b = 24.15 Å c = 3.85 Å α = β = γ = 90°	*P1*	Rwp = 1.21 % Rp = 1.09 %
NQ-COF$_{F1}$	a = 37.68 Å b = 36.15 Å c =3.62 Å α = β = 90° γ = 120°	*P1*	Rwp = 1.34 % Rp = 1.17 %
NQ-COF$_{F2}$	a = 34.21 Å b = 36.72 Å c = 4.92 Å α = β = 90° γ = 120°	*P1*	Rwp = 4.60 % Rp = 3.61 %
NQ-COF$_{F3}$	a = 23.43 Å b = 23.82 Å c = 3.83 Å α = β = γ = 90°	*P1*	Rwp = 1.91 % Rp = 1.51 %
NQ-COF$_{G1}$	a = 37.30 Å b = 36.95 Å c = 3.79 Å α = β = 90° γ = 120°	*P1*	Rwp = 3.78 % Rp = 2.93 %

5. Typical procedures of the titration by Karl Fischer reagent:

10 μL (10 mg) of distilled water was added into the mixed solvent of dry mesitylene (0.5 mL) and dry dioxane (0.5 mL) in a 10 mL glass tube with a magnetic stirring bar. Karl Fischer reagent was then dropped into the above mixed solvent, and the titration was stopped until the endpoint was reached (Supplementary Fig. 1). The amount of water was determined according to equation: $T = M/V_{KF}$, in which V_{KF} (mg/mL) represents the consumed volume of Karl Fisher reagent while M is the exact mass of water. The value of Average T was calculated to be 6.65 mg/mL after 5 parallel tests (Supplementary Table 4).

Supplementary Fig. 1 Digital photo of titration set-up by Karl Fischer reagent.

Supplementary Table 4. Titration by Karl Fischer reagents

V1 (mL)	V2 (mL)	V_{KF} (mL)	T (mg/mL)	T (Average)
3.09	4.58	1.49	6.71	6.65
4.58	6.09	1.51	6.62	
6.09	7.59	1.5	6.67	
7.59	9.1	1.51	6.62	
9.1	10.61	1.51	6.62	

Determination of water in the process of synthesizing NQ-COF$_{A1}$-OPR:

Batch A: NQ-COF$_{A1}$-OPR were prepared in the optimized conditions in the presence of $MgSO_4$. As the reaction finished, 1 mL of supernatant was taken after being centrifuged and added into a glass tube. Following the typical titration procedure, the average content of water was determined to be 0.89 mg/mL (Supplementary Table 5).

Batch B: NQ-COF$_{A1}$-OPR were prepared in the optimized conditions without addition of $MgSO_4$. Following the above process, the content of water was determined to be 2.36 mg/mL (Supplementary Table 6).

Supplementary Table 5. Titration for **COF$_{A1}$** in the presence of $MgSO_4$.

V1 (mL)	V2 (mL)	V_{KF} (mL)	T (mg/mL)	T (Average)
13.27	13.41	0.14	0.62	0.59
13.41	13.54	0.13	0.58	
13.54	13.67	0.13	0.57	
13.67	13.81	0.14	0.62	
13.81	13.94	0.13	0.58	

Supplementary Table 6. Titration for **NQ-COF$_{A1}$-OPR** in the absence of $MgSO_4$.

V1 (mL)	V2 (mL)	V_{KF} (mL)	T (mg/mL)	T (Average)
10.61	11.14	0.53	2.35	2.36
11.14	11.68	0.54	2.395	
11.68	12.2	0.52	2.31	
12.2	12.73	0.53	2.35	
12.73	13.27	0.54	2.39	

6. Characterization of NQ-COFs

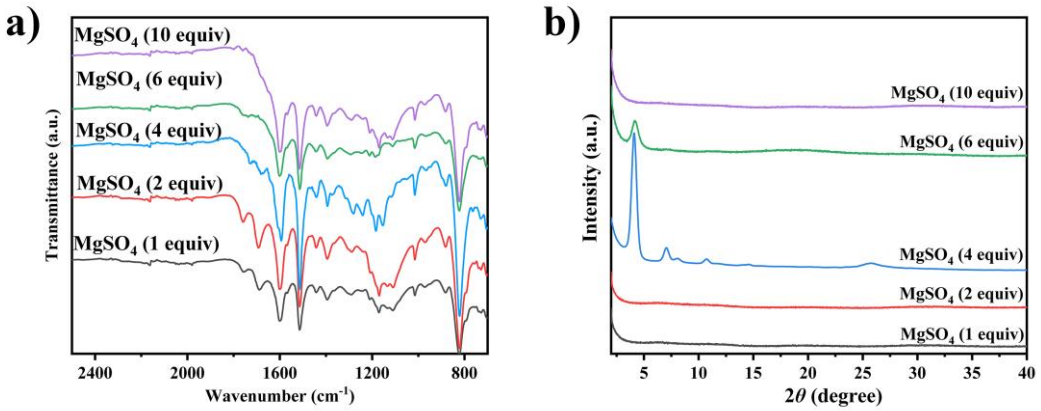

Supplementary Fig. 2 Characterization of **NQ-COF$_{A1}$-OPR** with different amount of $MgSO_4$. (a) FT-IR and (b) PXRD patterns.

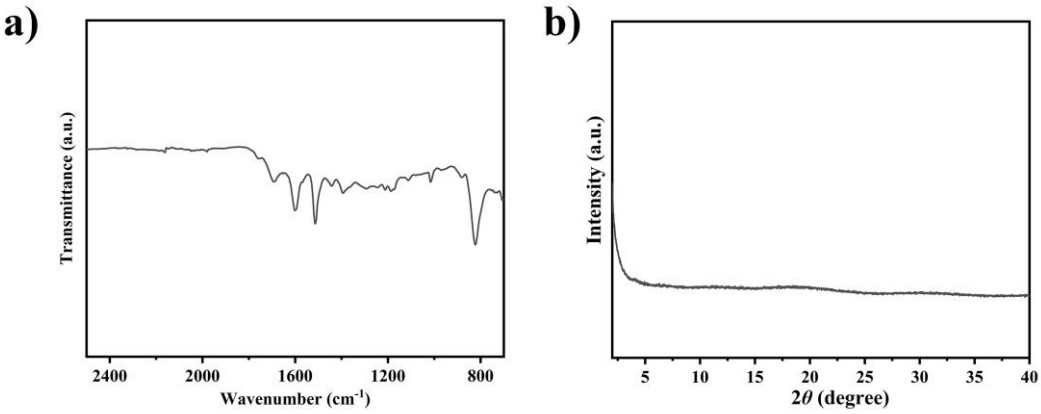

Supplementary Fig. 3 Characterization of **NQ-COF$_{A1}$-OPR** in the presence of $CaCl_2$.

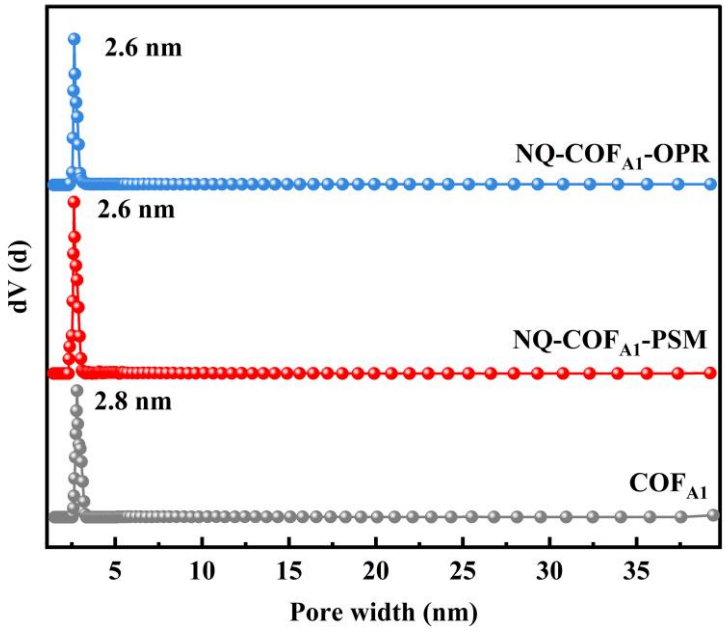

Supplementary Fig. 4 Pore size distribution profiles of **COF$_{A1}$**, **NQ-COF$_{A1}$-PSM**, and **NQ-COF$_{A1}$-OPR**.

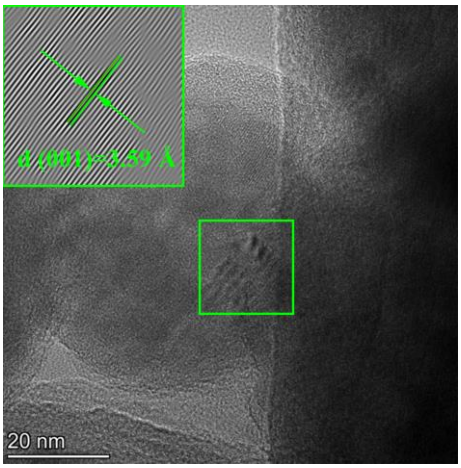

Supplementary Fig. 5 HRTEM image of **NQ-COF$_{A1}$-OPR** (the inset shows the enlarged image of the selected area).

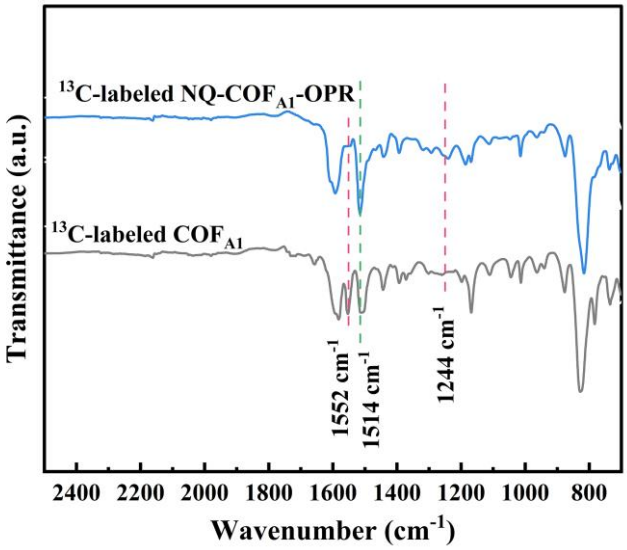

Supplementary Fig. 6 FT-IR spectra of isotopically ^{13}C-labelled **COF$_{A1}$** and **NQ-COF$_{A1}$-OPR**.

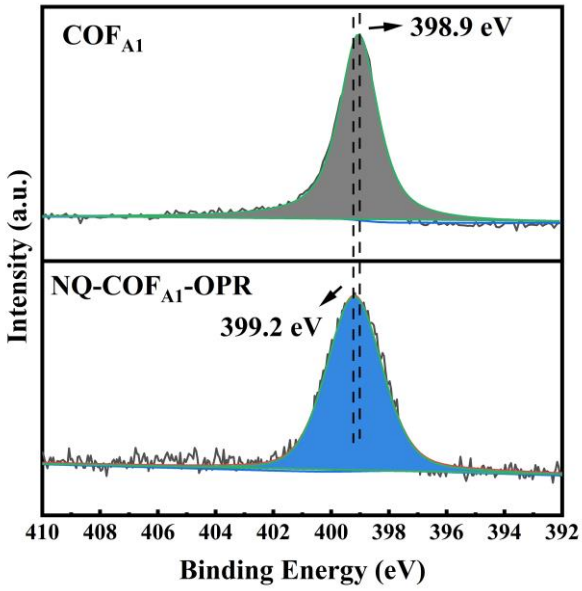

Supplementary Fig. 7 High resolution N 1s XPS spectra of **COF$_{A1}$** and **NQ-COF$_{A1}$-OPR**.

.

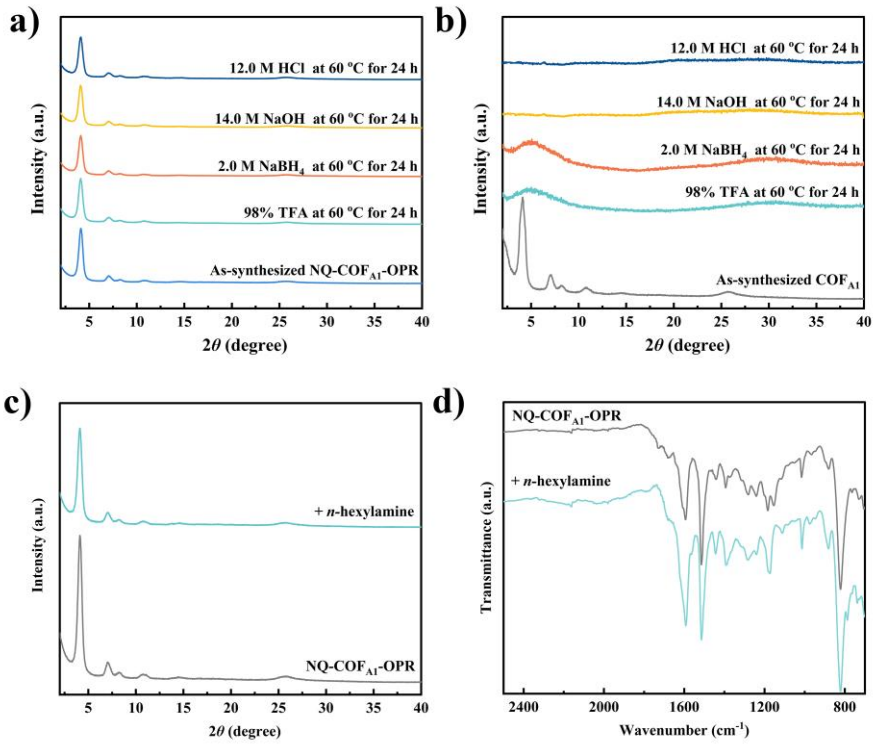

Supplementary Fig. 8 Chemical stability test. PXRD patterns of (a) **NQ-COF$_{A1}$-OPR** and (b) **COF$_{A1}$** after treatment under different harsh chemical conditions. (c) PXRD patterns and (d) FT-IR spectra of **NQ-COF$_{A1}$-OPR** before and after treatment in n-hexylamine solution for 24 h.

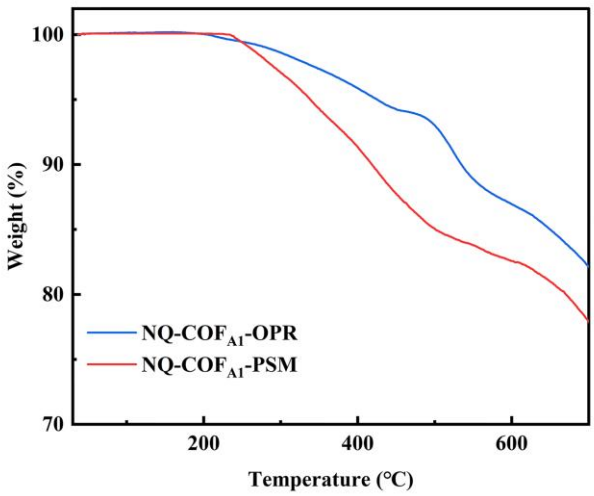

Supplementary Fig. 9 Thermal stability evaluation by TGA measurement.

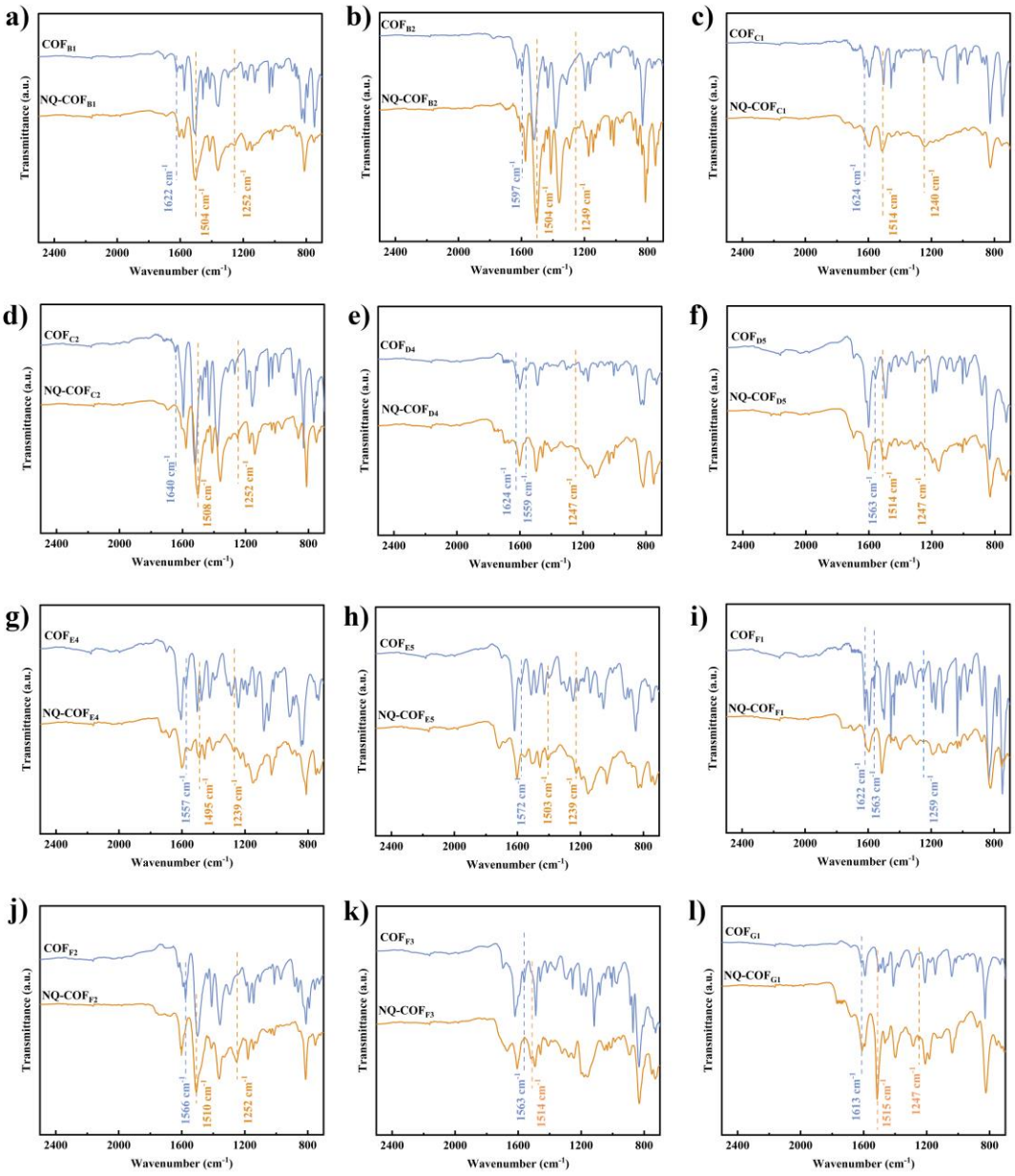

Supplementary Fig. 10 FT-IR spectra of different COFs and NQ-COFs.

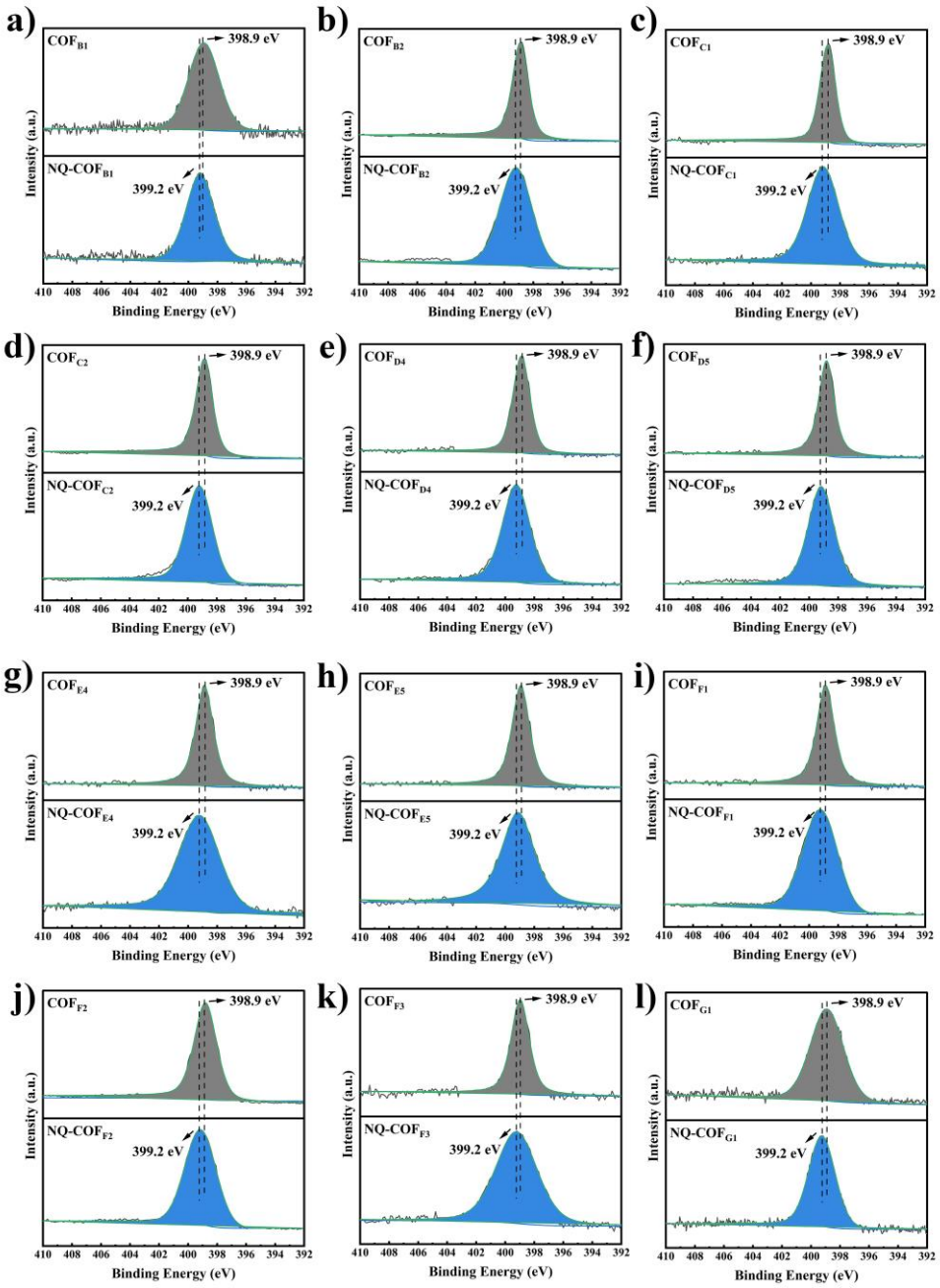

Supplementary Fig. 11 High resolution N 1s XPS spectra of NQ-COFs and corresponding imine-linked COFs.

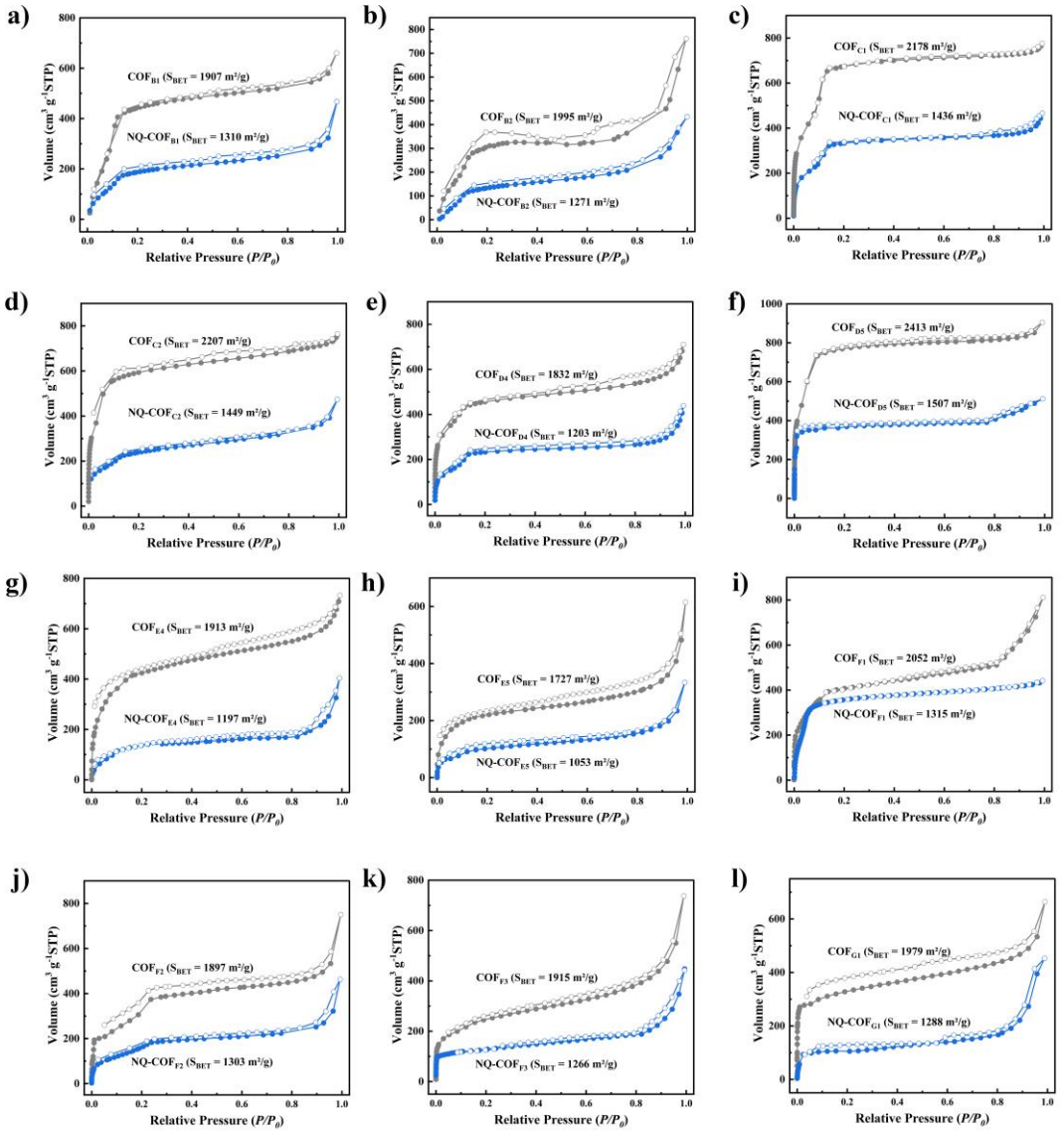

Supplementary Fig. 12 N_2 sorption isotherm curves of NQ-COFs and corresponding imine-linked COFs.

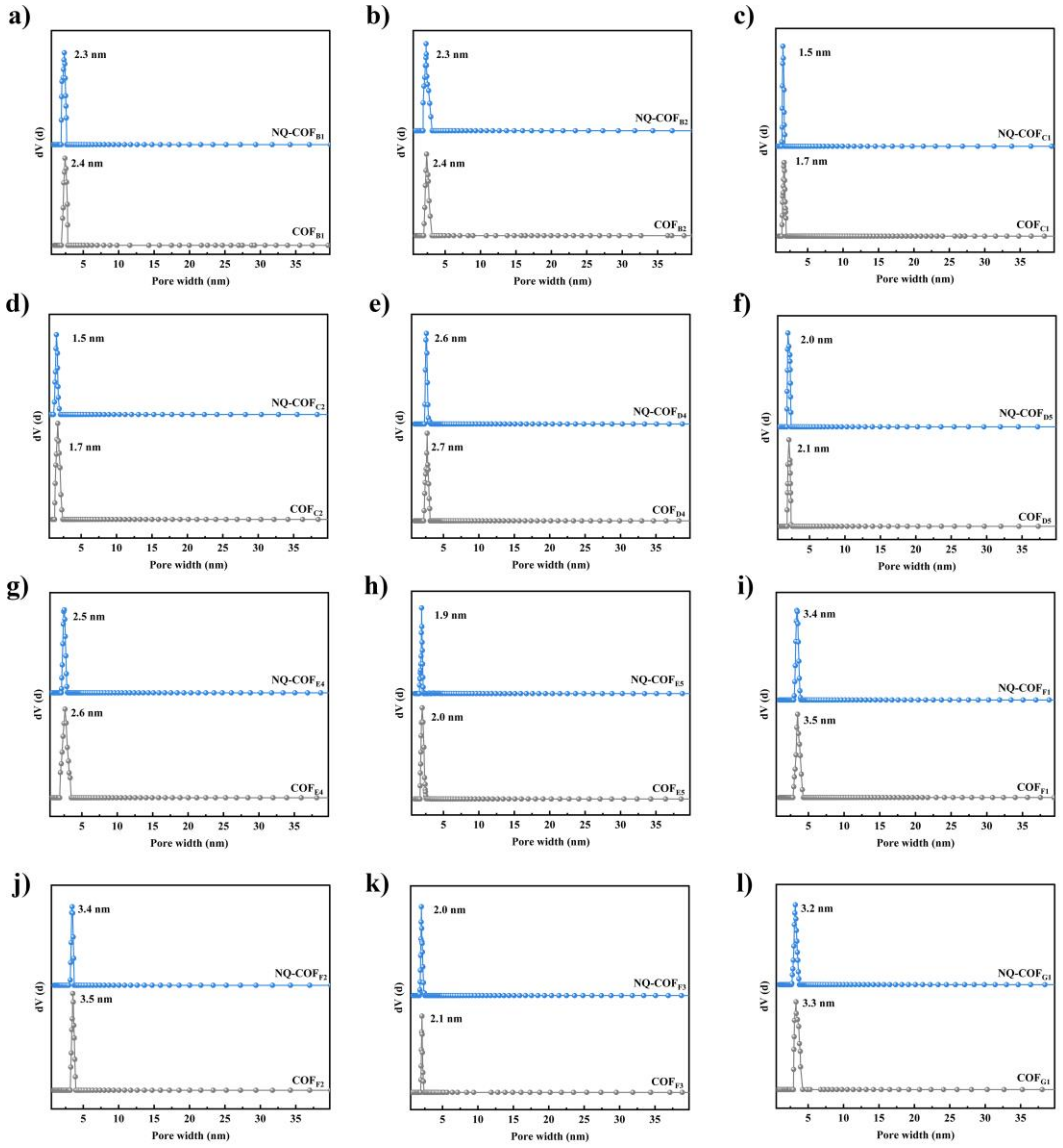

Supplementary Fig. 13 Pore size distribution profiles of NQ-COFs and corresponding imine-linked COFs.

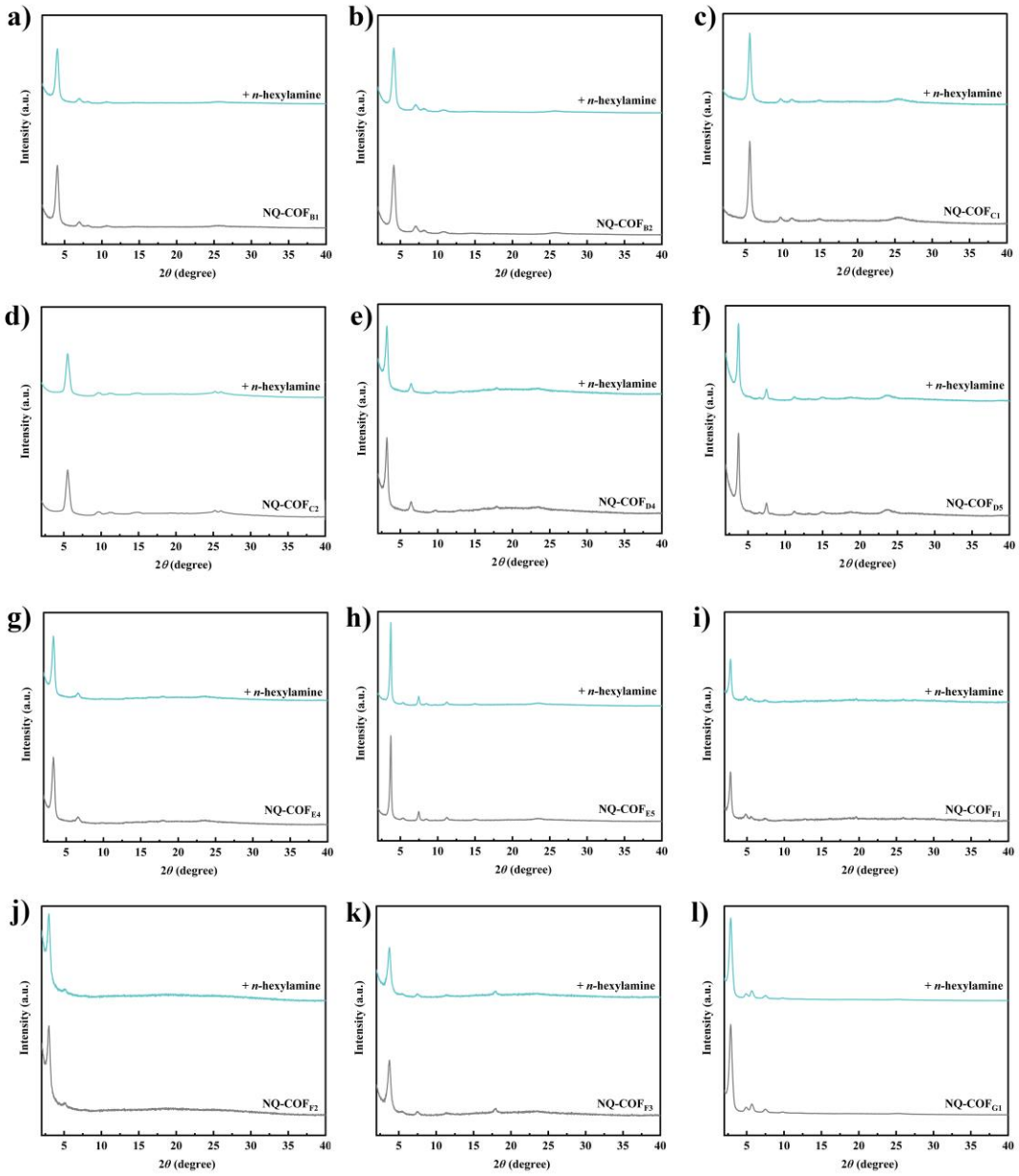

Supplementary Fig. 14 PXRD patterns of different NQ-COFs before and after treatment in *n*-hexylamine solution for 24 h.

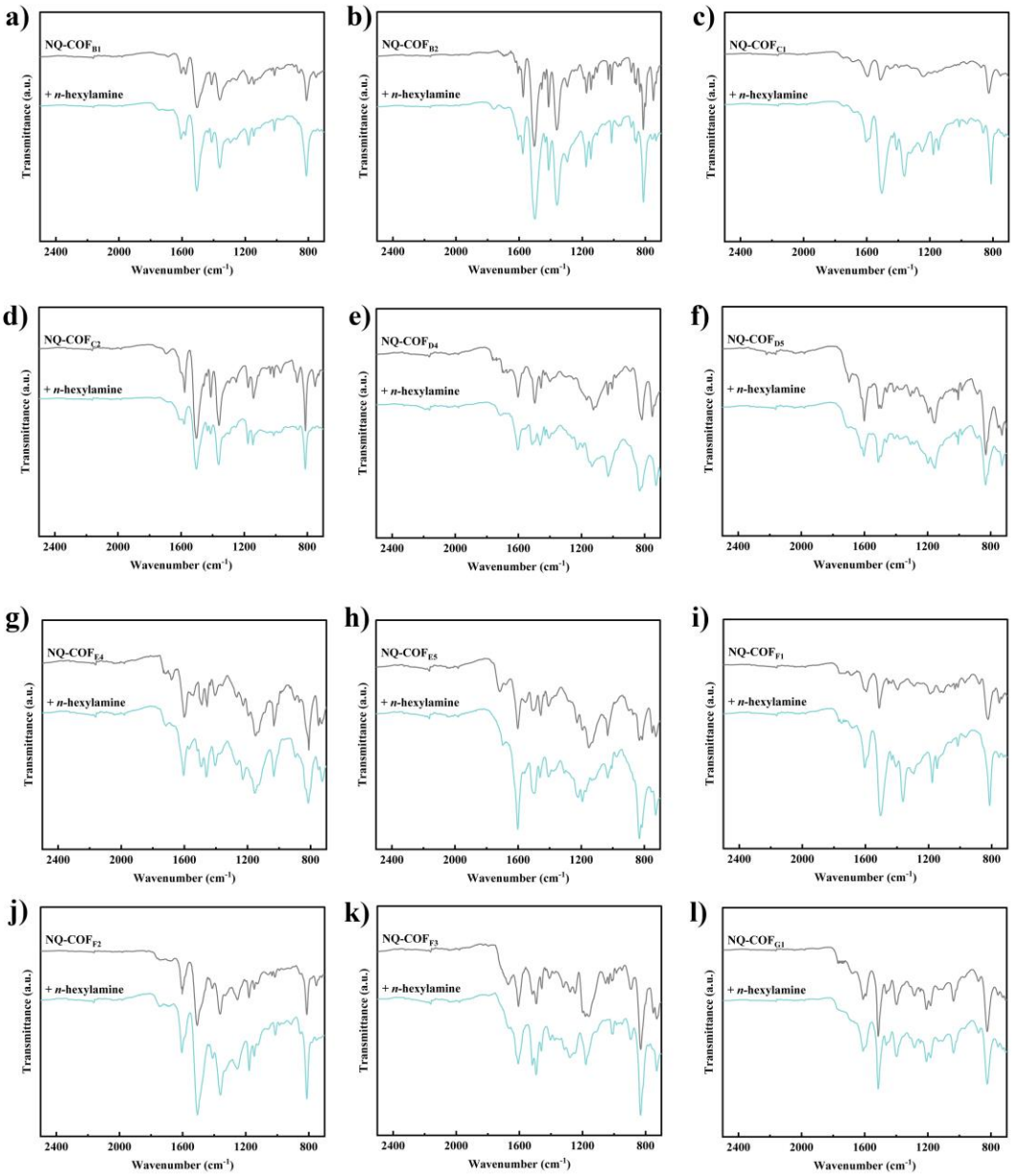

Supplementary Fig. 15 FT-IR spectra of different COFs and NQ-COFs before and after treatment in *n*-hexylamine solution for 24 h.

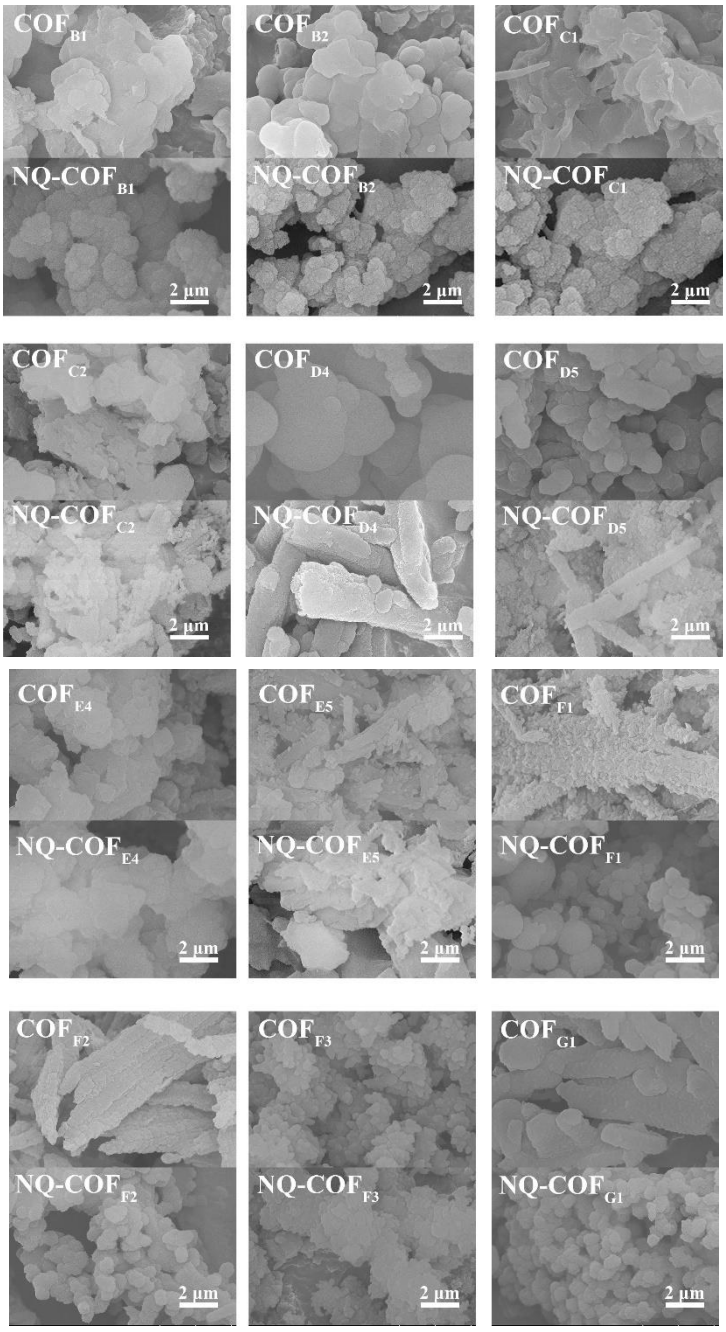

Supplementary Fig. 16 SEM images of NQ-COFs and corresponding imine-linked COFs.

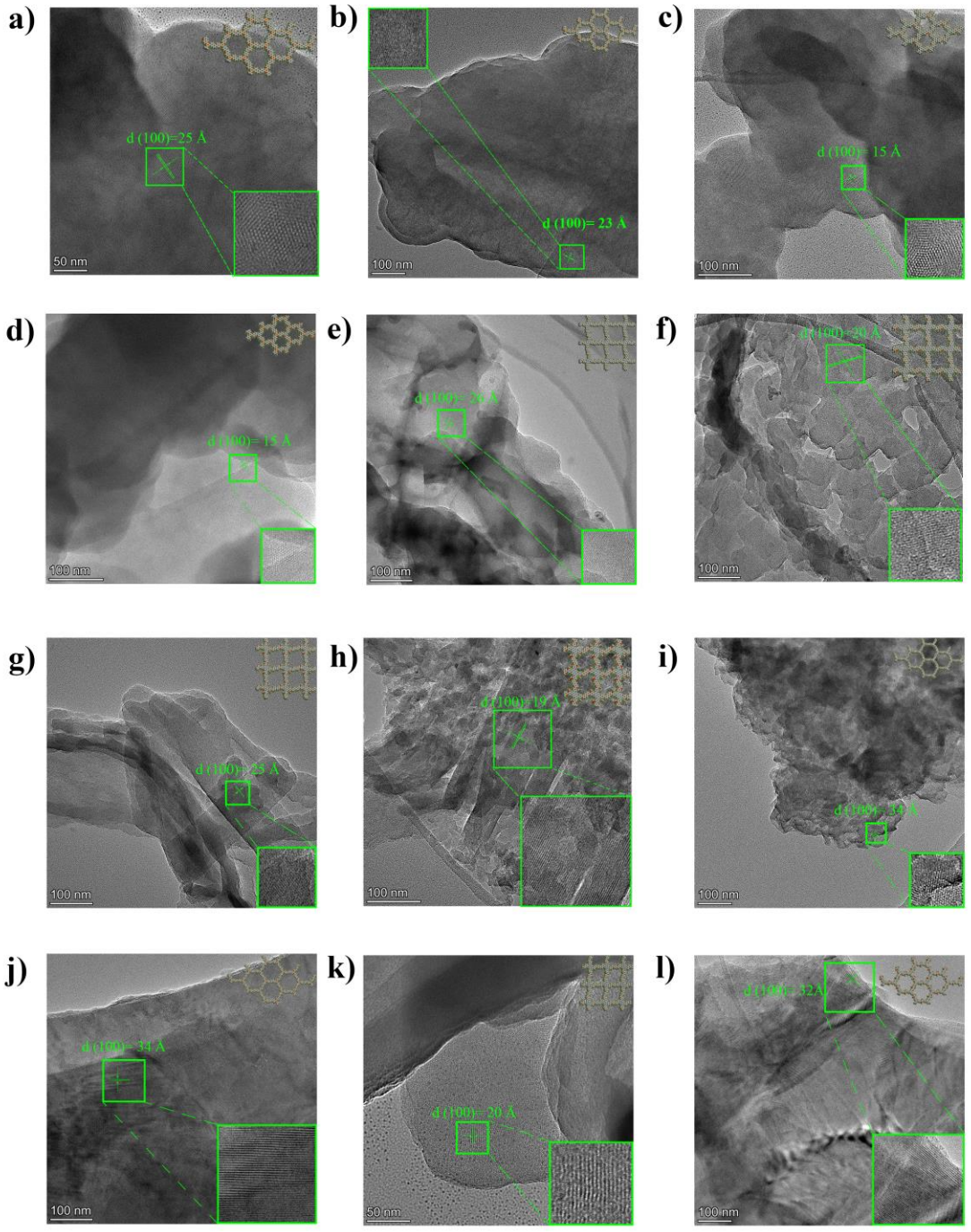

Supplementary Fig. 17 HRTEM images of (a) **NQ-COF$_{B1}$**, (b) **NQ-COF$_{B2}$**, (c) **NQ-COF$_{C1}$**, (d) **NQ-COF$_{C2}$**, (e) **NQ-COF$_{D4}$**, (f) **NQ-COF$_{D5}$**, (g) **NQ-COF$_{E4}$** (h) **NQ-COF$_{E5}$**, (i) **NQ-COF$_{F1}$**, (j) **NQ-COF$_{F2}$** (k) **NQ-COF$_{F3}$** and (l) **NQ-COF$_{G1}$**. The insets show the enlarged image of the selected area.

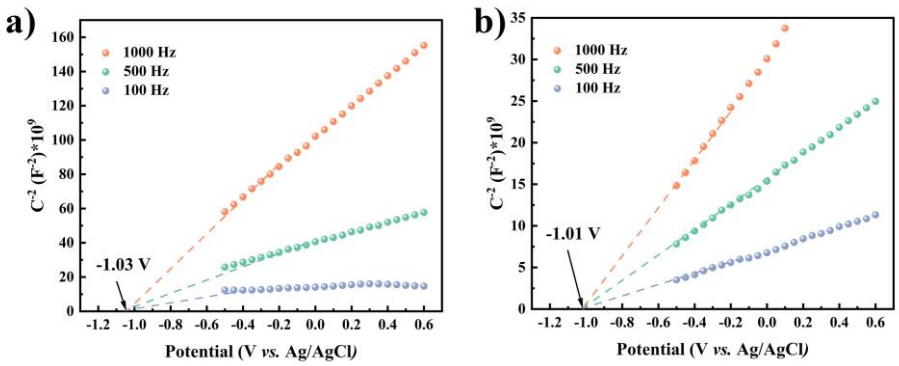

Supplementary Fig. 18 Mott-Schottky plots of (a) **COF_{A1}** and (b) **NQ-COF_{A1}-PSM**.

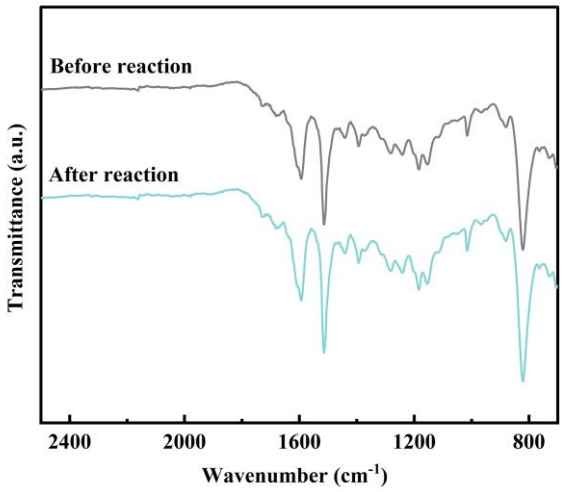

Supplementary Fig. 19 FT-IR spectra of **NQ-COF_{A1}-OPR** before and after the five runs of the photocatalytic reaction.

7. Photocatalytic synthesis of 2-benzimidazole based derivatives

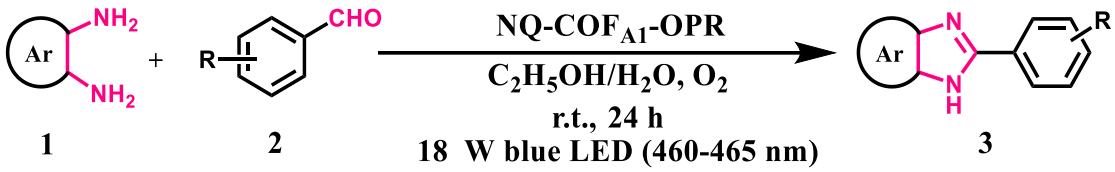

1 2 3

Detection of H_2O_2:

The generation of H_2O_2 in the photocatalytic reaction was detected by the following mechanism:

$$H_2O_2 + 2KI + H_2SO_4 \rightarrow I_2 + K_2SO_4 + 2H_2O$$

Typical procedure: after finishing the synthesis of 2-phenyl-1*H*-benzo[*d*]imidazole (**3a**), 0.5 mL aliquot of the filtrate was diluted with 5 mL distilled water. Subsequently, 5 mL of 3.5 M H_2SO_4 solution, 1 mL of 0.1 M KI solution, and 1 mL of 0.4 M Potassium biphthalate solution were successively added to the above solution to evaluate the generation of H_2O_2.

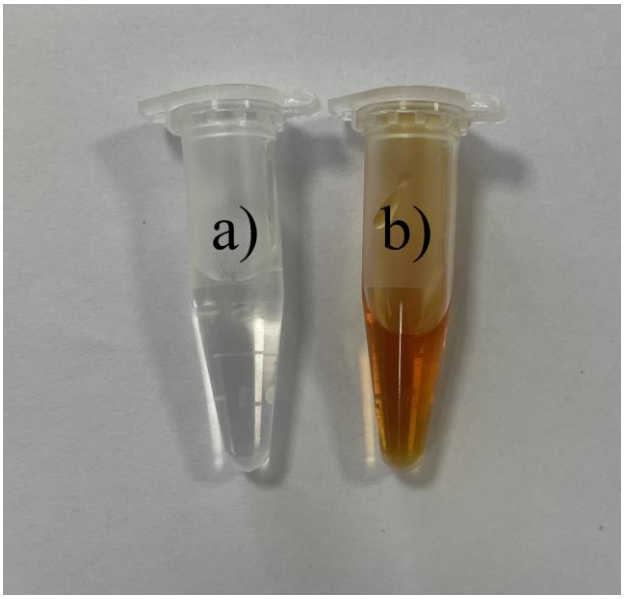

Supplementary Fig. 20 (a) Photo image of potassium iodide, potassium biphthalate, and 3.5 M H_2SO_4 mixture solution, which was changed to dark yellow (b) after addition

of 0.5 mL aliquot of the filtrate 3a.

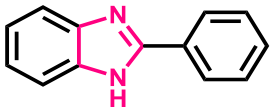

2-phenyl-1*H*-benzo[*d*]imidazole (3a): 96 mg, 0.495 mmol, 99 % yield. ^{1}H NMR (600 MHz, DMSO-d$_6$) δ 12.93 (br s, 1H), 8.19 (d, *J* = 7.2 Hz, 2H), 7.61 (s, 2H), 7.56-7.48 (m, 3H), 7.22-7.19 (m, 2H); ^{13}C NMR (151 MHz, DMSO-d$_6$) δ 151.2, 130.1, 129.9, 128.9, 126.4, 122.1.

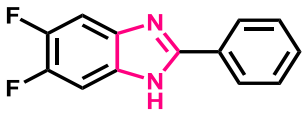

5,6-difluoro-2-phenyl-1*H*-benzo[*d*]imidazole (3b): 108 mg, 0.47 mmol, 94 % yield. ^{1}H NMR (600 MHz, DMSO-d$_6$) δ 13.17 (br s, 1H), 8.15 (d, *J* = 8.4 Hz, 2H), 7.68-7.49 (m, 5H); ^{13}C NMR (151 MHz, DMSO-d$_6$) δ 153.3, 130.2, 129.7, 129.0, 126.4; ^{19}F NMR (564 MHz, DMSO-d$_6$): δ -140.9, -142.9.

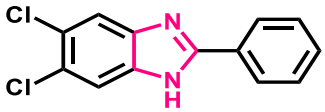

5,6-dichloro-2-phenyl-1*H*-benzo[*d*]imidazole (3c): 115 mg, 0.44 mmol, 88 % yield. ^{1}H NMR (600 MHz, DMSO-d$_6$) δ 13.26 (br s, 1H), 8.17 (d, *J* = 8.4 Hz, 2H), 7.94 (s, 1H), 7.76 (s, 1H),7.59-7.52 (m, 3H); ^{13}C NMR (151 MHz, DMSO-d$_6$) δ 154.3, 131.1, 129.7, 125.6, 127.2.

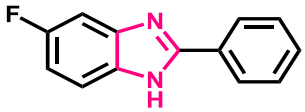

5-fluoro-2-phenyl-1*H*-benzo[*d*]imidazole (3d): 87 mg, 0.41 mmol, 82 % yield. ^{1}H NMR (600 MHz, DMSO-d$_6$) δ 13.05 (br s, 1H), 8.17 (d, *J* = 7.4 Hz, 2H),7.69-7.33 (m, 5H), 7.06 (s, 1H); ^{13}C NMR (151 MHz, DMSO-d$_6$) δ 159.7, 158.1, 152.9, 131.7, 130.1,

128.8, 126.5, 119.7, 111.9, 110.6, 104.4. ^{19}F NMR (564 MHz, DMSO-d$_6$) δ -119.6, -121.4.

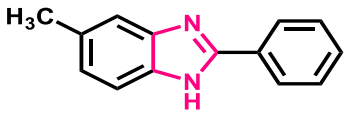

5-methyl-2-phenyl-1*H*-benzo[*d*]imidazole (3e): 89 mg, 0.43 mmol, 85 % yield. ^{1}H NMR (600 MHz, DMSO-d$_6$) δ 12.74 (br s, 1H), 8.16 (d, *J* = 7.1 Hz, 2H),7.63-7.32 (m, 5H), 7.03 (s, 1H); ^{13}C NMR (151 MHz, DMSO-d$_6$) δ 133.3, 130.8, 130.1, 129.7, 129.4, 126.8, 119.0, 111.5, 21.8.

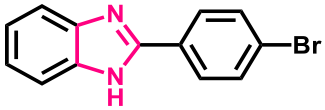

2-(4-bromophenyl)-1*H*-benzo[*d*]imidazole (**3f**): 121 mg, 0.45 mmol, 89 % yield. ^{1}H NMR (600 MHz, DMSO-d$_6$) δ 12.96 (br s, 1H), 8.12 (d, *J* = 7.8 Hz, 2H), 7.76 (d, *J* = 8.4 Hz, 2H), 7.60 (s, 2H), 7.34-7.20 (m, 2H); ^{13}C NMR (151 MHz, DMSO-d$_6$) δ 150.7, 132.4, 129.9, 128.8, 123.7, 122.8.

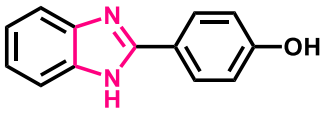

4-(1*H*-benzo[*d*]imidazol-2-yl) phenol (3g): 96 mg, 0.46 mmol, 92 % yield. ^{1}H NMR (600 MHz, DMSO-d$_6$) δ 12.65 (br s, 1H), 9.98 (s, 1H), 8.01 (d, *J* = 8.4Hz, 2H), 7.54 (s, 2H), 7.16-7.14 (m, 2H), 6.92 (d, *J* = 8.4 Hz, 2H); ^{13}C NMR (151 MHz, DMSO-d$_6$) δ 159.6, 152.3, 128.6, 122.1, 121.6, 116.1.

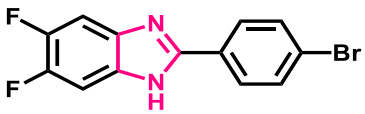

2-(4-bromophenyl)-5,6-difluoro-1*H*-benzo[*d*]imidazole (**3h**): 144 mg, 0.47 mmol, 94 % yield. ^{1}H NMR (600 MHz, DMSO-d$_6$) δ 13.26 (br s, 1H), 8.08 (d, *J* = 8.6 Hz,

2H), 7.77 (d, J = 8.6 Hz, 2H), 7.65 (s, 2H); ^{13}C NMR (151 MHz, DMSO-d$_6$) δ 152.7, 132.5, 129.3, 128.8, 124.1; ^{19}F NMR (564 MHz, DMSO-d$_6$) δ -143.0, -144.8.

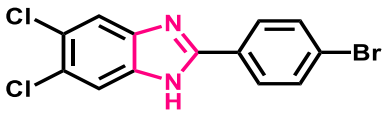

2-(4-bromophenyl)-5,6-chloro-1*H*-benzo[*d*]imidazole (**3i**): 137 mg, 0.40 mmol, 80 % yield. ^{1}H NMR (600 MHz, DMSO-d$_6$) δ 13.36 (br s, 1H), 8.10 (d, J = 8.4 Hz, 2H), 7.87-7.78 (m, 4H); ^{13}C NMR (151 MHz, DMSO-d$_6$) δ 153.3, 132.6, 129.1, 128.9, 124.5.

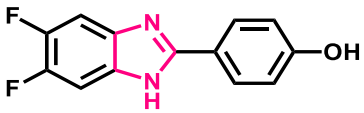

4-(5,6-difluoro-1*H*-benzo[*d*]imidazol-2-yl) phenol (**3j**): 109 mg, 0.45 mmol, 89 % yield. ^{1}H NMR (600 MHz, DMSO-d$_6$) δ 12.91 (br s, 1H), 10.04 (s, 1H), 7.96 (d, J = 7.0 Hz, 2H), 7.57 (s, 2H), 6.91 (d, J = 7.0 Hz, 2H); ^{13}C NMR (151 MHz, DMSO-d$_6$) δ 170.8, 159.8, 154.3, 147.8, 147.7, 146.2, 146.1, 128.6, 121.1, 116.2; ^{19}F NMR (564 MHz, DMSO-d$_6$) δ -144.5, -145.8.

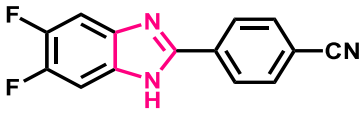

4-(5,6-difluoro-1*H*-benzo[*d*]imidazol-2-yl) benzonitrile (3k): 108 mg, 0.43 mmol, 85 % yield. ^{1}H NMR (600 MHz, DMSO-d$_6$) δ 13.41 (br s, 1H), 8.30 (d, J = 8.4 Hz, 2H), 8.03 (d, J = 8.3 Hz, 2H), 7.72 (s, 2H); ^{13}C NMR (151 MHz, DMSO-d$_6$) δ 134.2, 133.5, 127.5, 119.0, 112.6. ^{19}F NMR (564 MHz, DMSO-d$_6$) δ -141.8, -143.7.

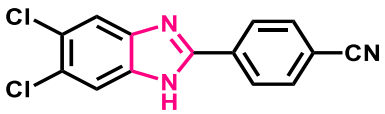

4-(5,6-dichloro-1*H*-benzo[*d*]imidazol-2-yl) benzonitrile (3l): 115 mg, 0.4 mmol, 80 % yield. ^{1}H NMR (600 MHz, DMSO-d$_6$) δ 13.55 (br s, 1H), 8.33 (d, J = 8.6 Hz, 2H), 8.05

(d, *J* = 8.6 Hz, 2H), 7.93 (s, 2H); ^{13}C NMR (151 MHz, DMSO-d$_6$) δ 152.5, 133.9, 133.6, 127.8, 113.0.

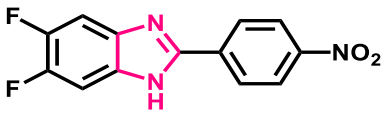

5,6-difluoro-2-(4-nitrophenyl)-1*H*-benzo[*d*]imidazole (3m): 114 mg, 0.42 mmol, 83 % yield. ^{1}H NMR (600 MHz, DMSO-d$_6$) δ 13.49 (br s, 1H), 8.41-8.37 (m, 2H), 7.73-7.70 (m, 2H), 5.75 (s, 2H); ^{13}C NMR (151 MHz, DMSO-d$_6$) δ 151.5, 148.4, 135.9, 127.9, 124.8. ^{19}F NMR (564 MHz, DMSO-d$_6$) δ -142.2, -144.1.

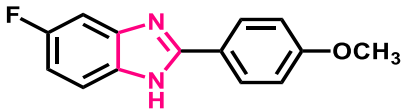

5-fluoro-2-(4-methoxyphenyl)-1*H*-benzo[*d*]imidazole (3n): 98 mg, 0.41 mmol, 81 % yield. ^{1}H NMR (600 MHz, DMSO-d$_6$) δ 12.87 (br s, 1H), 8.10 (s, 2H), 7.61-7.02 (m, 5H), 3.83 (s, 3H); ^{13}C NMR (151 MHz, DMSO-d$_6$) δ 161.2, 128.5, 122.9, 119.7, 114.9, 112.0, 110.5, 55.8. ^{19}F NMR (564 MHz, DMSO-d$_6$) δ -120.2, -121.8.

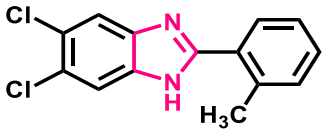

5,6-dichloro-2-(*o*-tolyl)-1*H*-benzo[*d*]imidazole (3o): 129 mg, 0.46 mmol, 93 % yield. ^{1}H NMR (600 MHz, DMSO-d$_6$) δ 12.97 (br s, 1H), 7.85 (s, 2H), 7.73 (d, *J* = 7.7 Hz, 1H), 7.44-7.37 (m, 3H), 2.59 (s, 3H); ^{13}C NMR (151 MHz, DMSO-d$_6$) δ 155.0, 137.7, 131.9, 130.4, 130.0, 129.6, 126.5, 21.4.

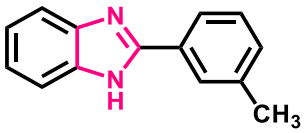

2-(m-tolyl)-1*H*-benzo[*d*]imidazole (3p): 93 mg, 0.44 mmol, 89 % yield. ^{1}H NMR (600

MHz, DMSO-d_6) δ 13.30 (br s, 1H), 8.09 (s, 1H), 8.03 (d, J = 7.7 Hz, 1H), 7.60-7.58 (m, 2H), 7.42-7.40 (t, 1H), 7.28 (d, J = 7.5 Hz, 1H), 7.19-7.17 (m, 2H), 2.40 (s, 3H); ^{13}C NMR (151 MHz, DMSO-d_6) δ 151.8, 138.5, 130.9, 130.6, 129.3, 127.6, 124.2, 122.4, 21.5.

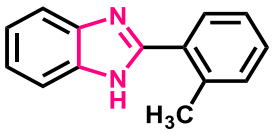

2-(*o*-tolyl)-1*H*-benzo[*d*]imidazole (3q): 96 mg, 0.46 mmol, 92 % yield. ^{1}H NMR (600 MHz, DMSO-d_6) δ 12.61 (br s, 1H), 7.74 (d, J = 7.4 Hz, 1H), 7.68 (d, J = 7.8 Hz, 1H), 7.52 (d, J = 7.7 Hz, 1H), 7.40-7.36 (m, 3H), 7.23-7.19 (m, 2H), 2.61 (s, 3H); ^{13}C NMR (151 MHz, DMSO-d_6) δ 152.4, 144.2, 137.5, 134.9, 131.7, 130.5, 129.9, 129.8, 126.4, 122.8, 121.9, 119.4, 111.7, 21.5.

8. Copies of NMR spectra

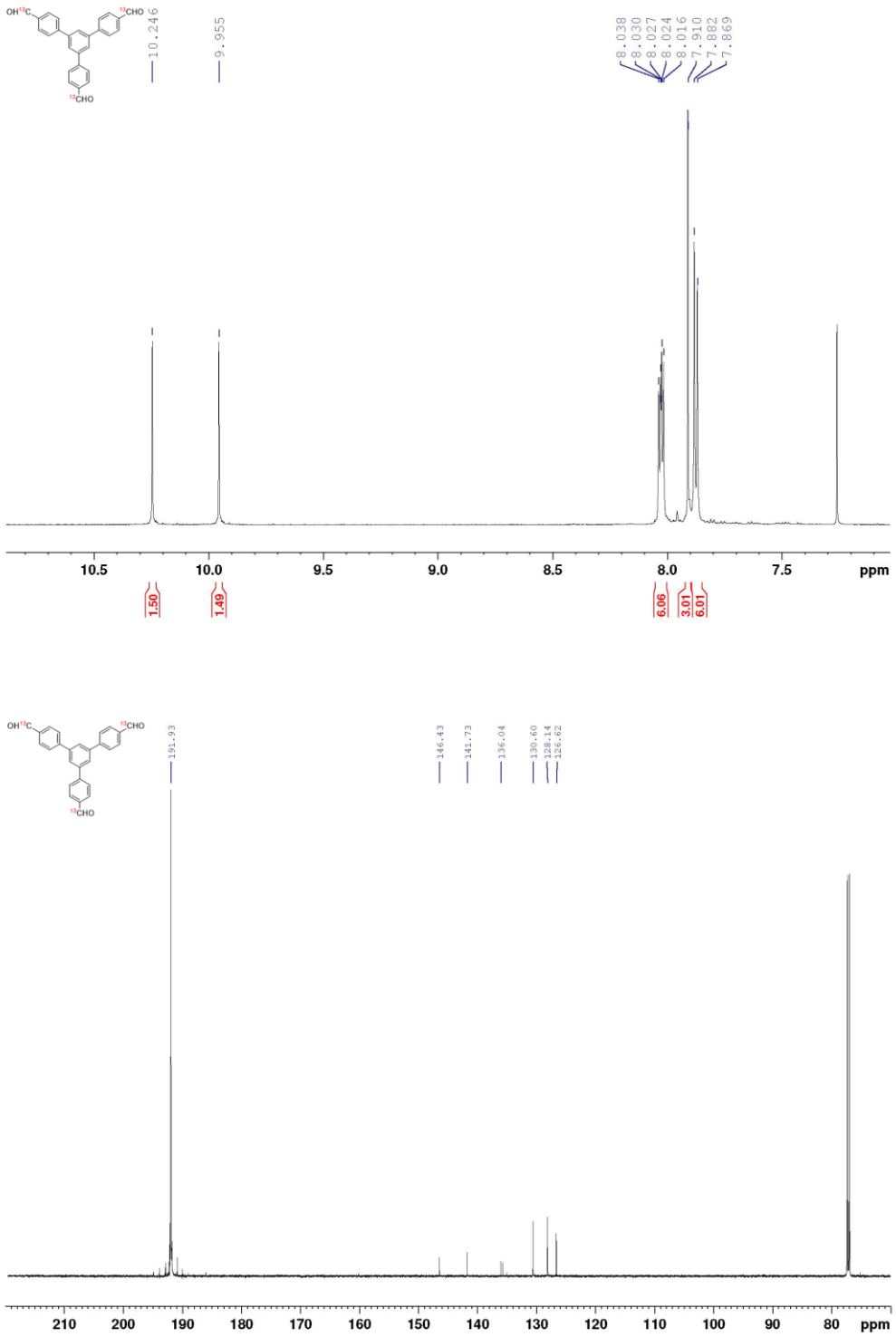

Supplementary Fig. 21 ^{1}H NMR and ^{13}C NMR spectra of **^{13}C-labeled A**.

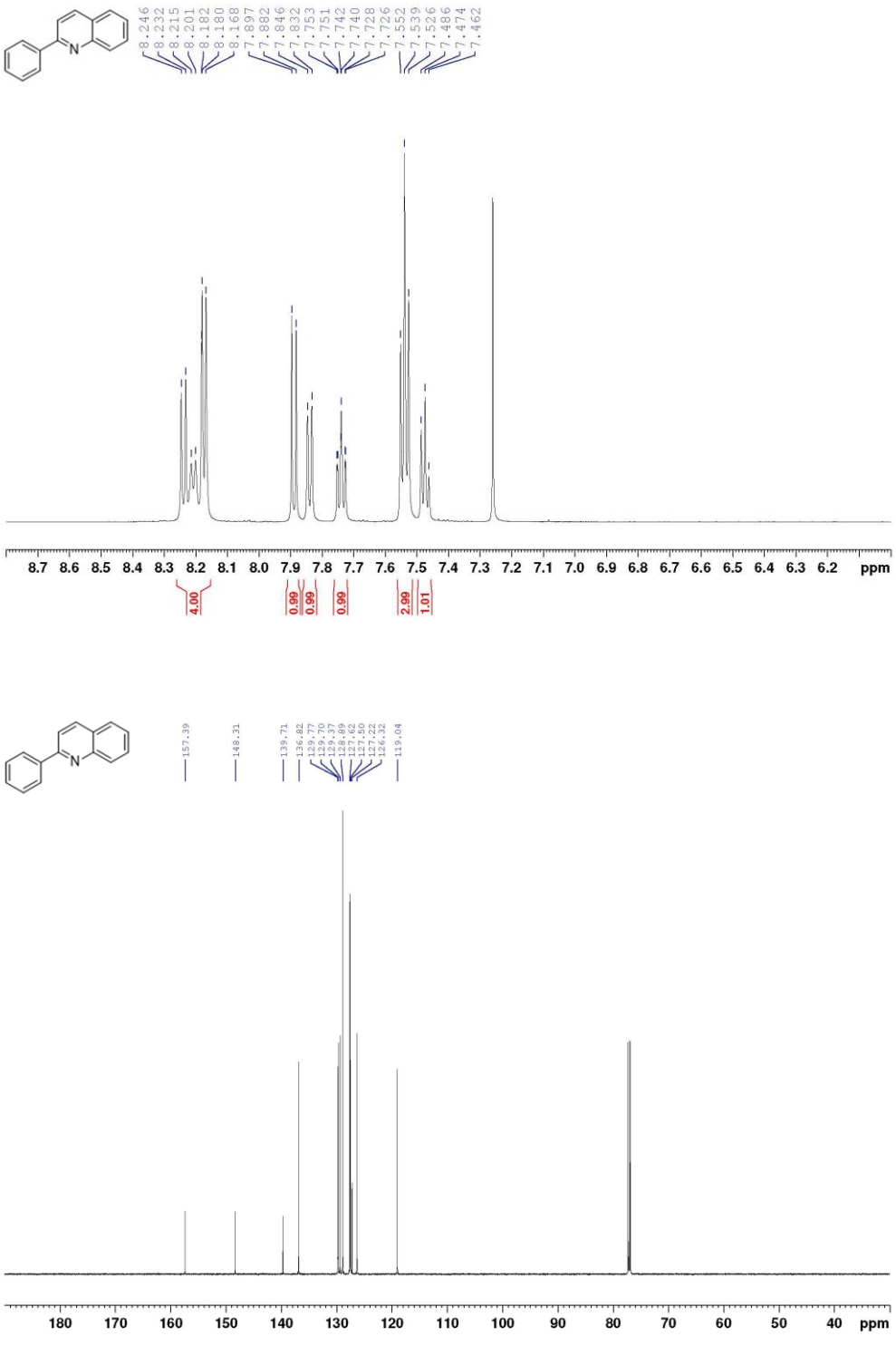

Supplementary Fig. 22 ^{1}H NMR and ^{13}C NMR spectra of 2-phenylquinoline.

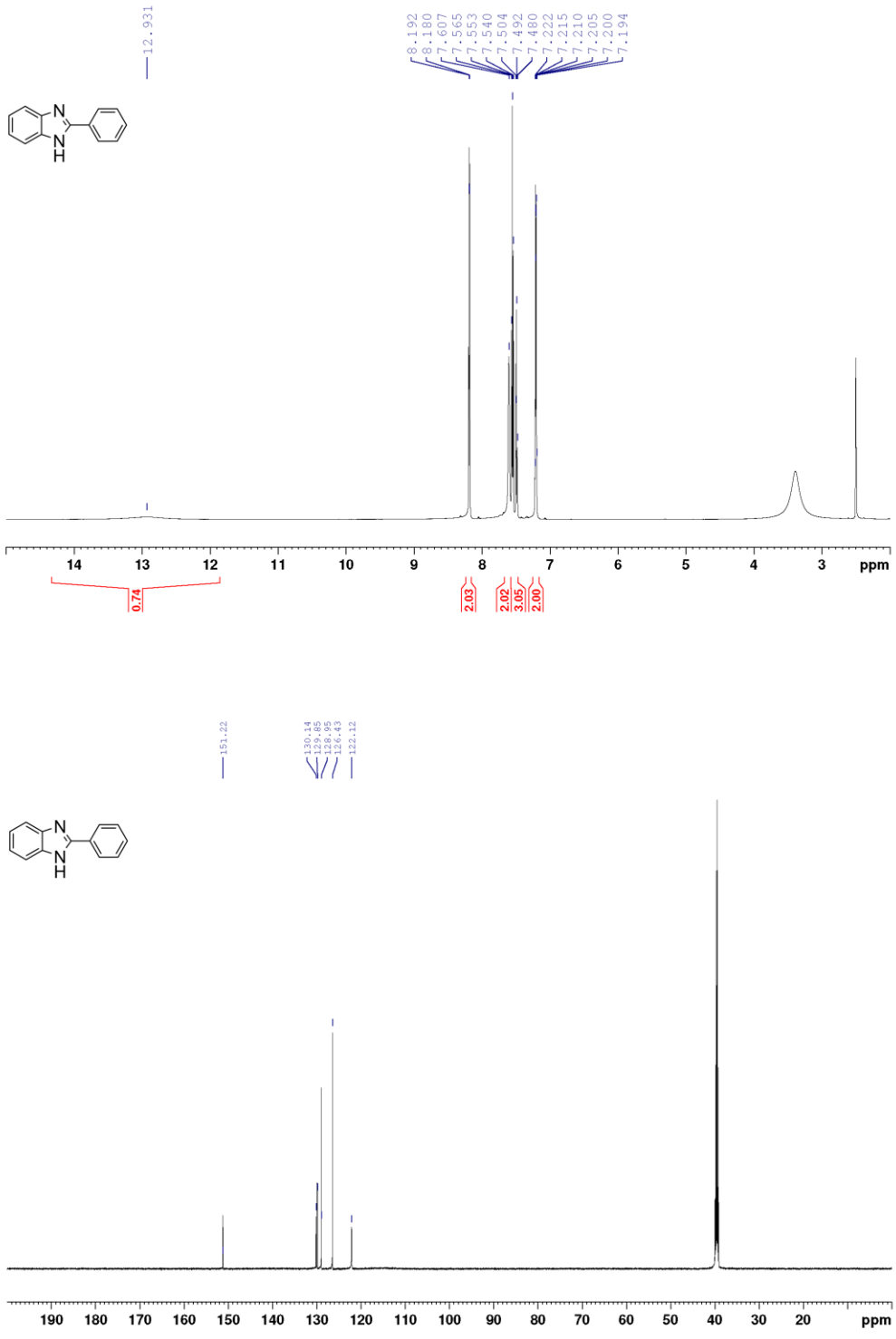

Supplementary Fig. 23 ^{1}H NMR and ^{13}C NMR spectra of **3a**.

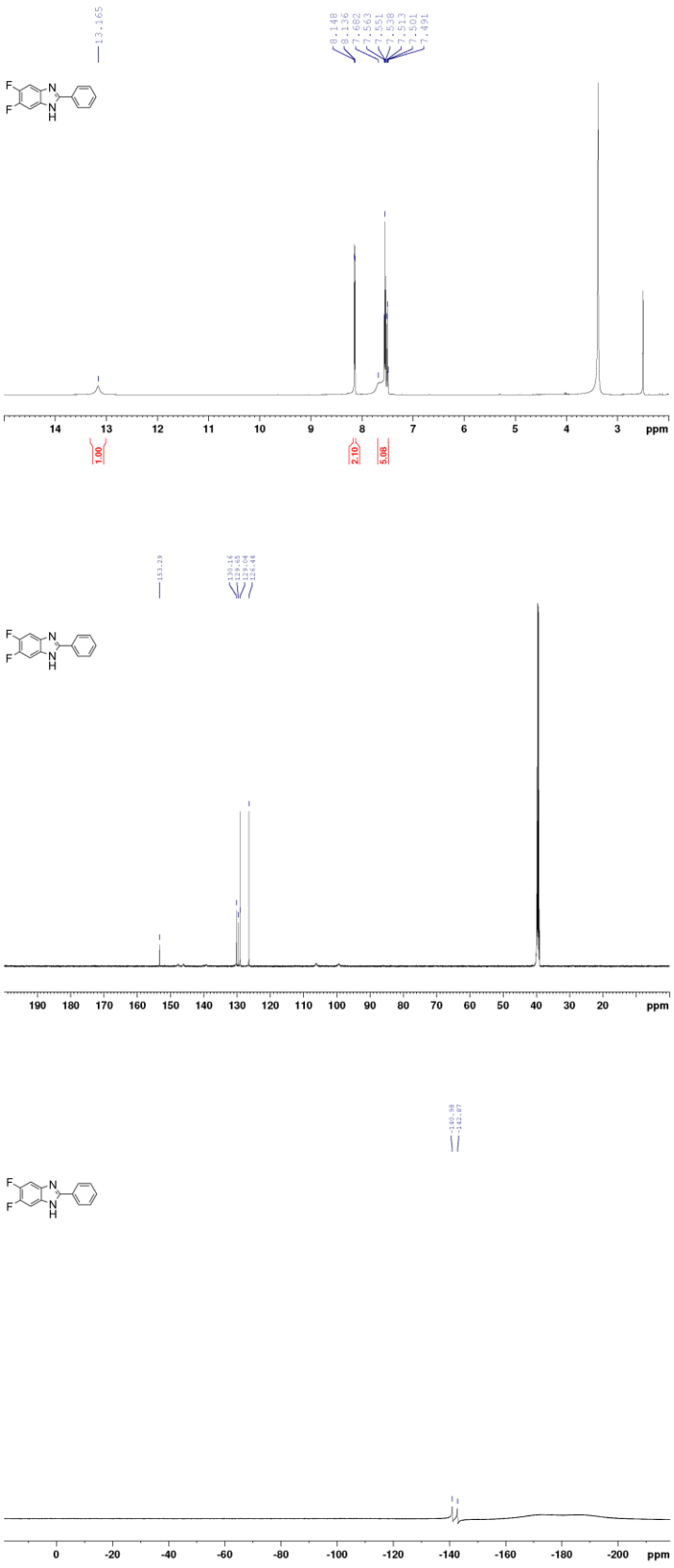

Supplementary Fig. 24 ^{1}H NMR, ^{13}C NMR, and ^{19}F NMR spectra of **3b**.

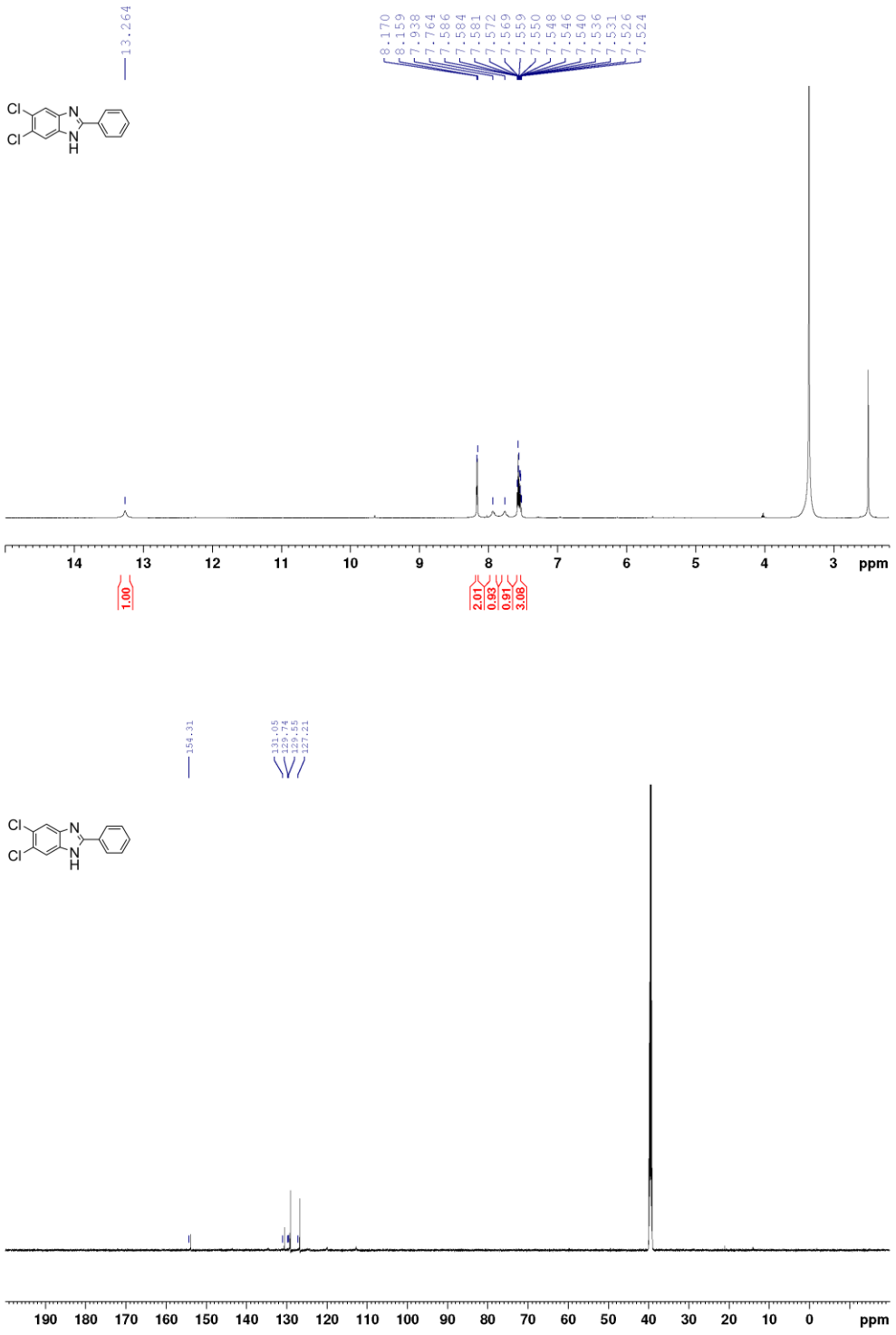

Supplementary Fig. 25 ^{1}H NMR and ^{13}C NMR spectra of **3c**.

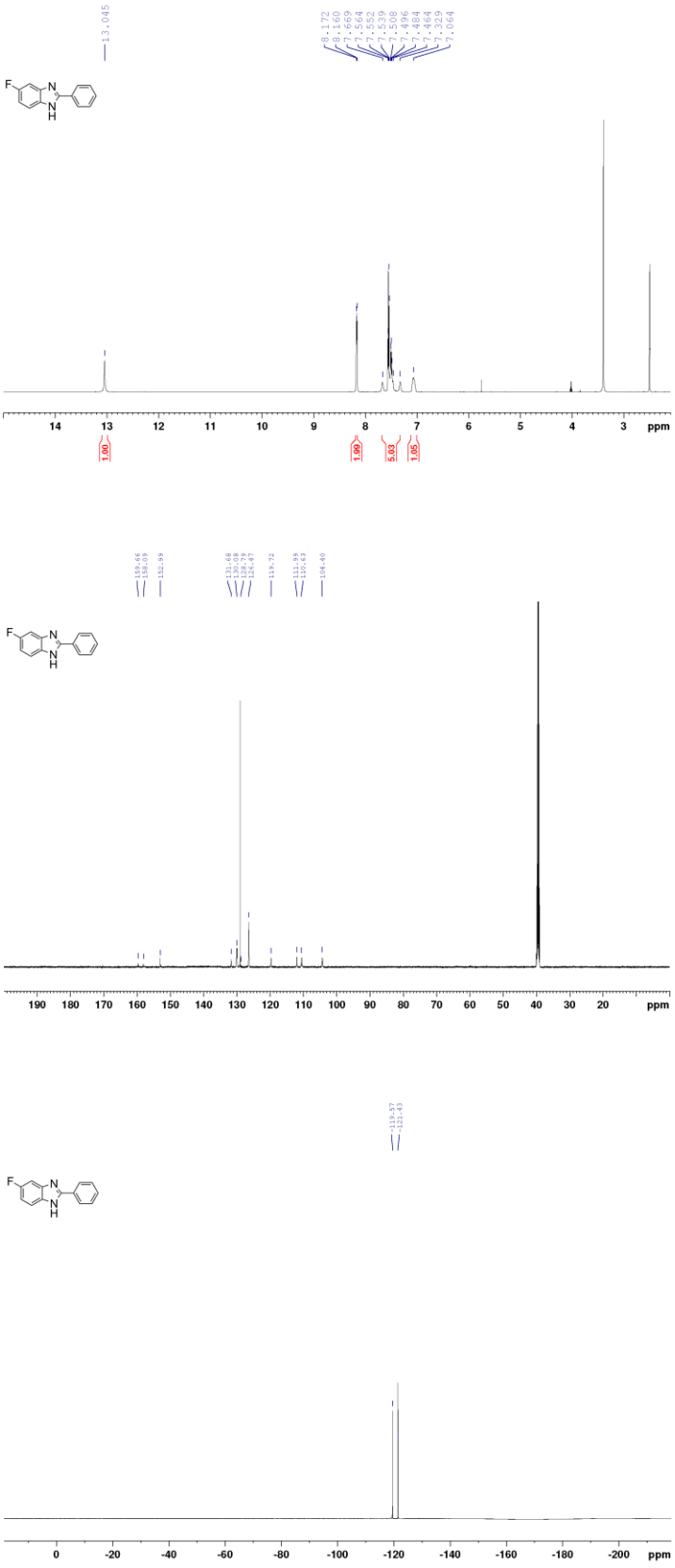

Supplementary Fig. 26 ^{1}H NMR, ^{13}C NMR, and ^{19}F NMR spectra of **3d**.

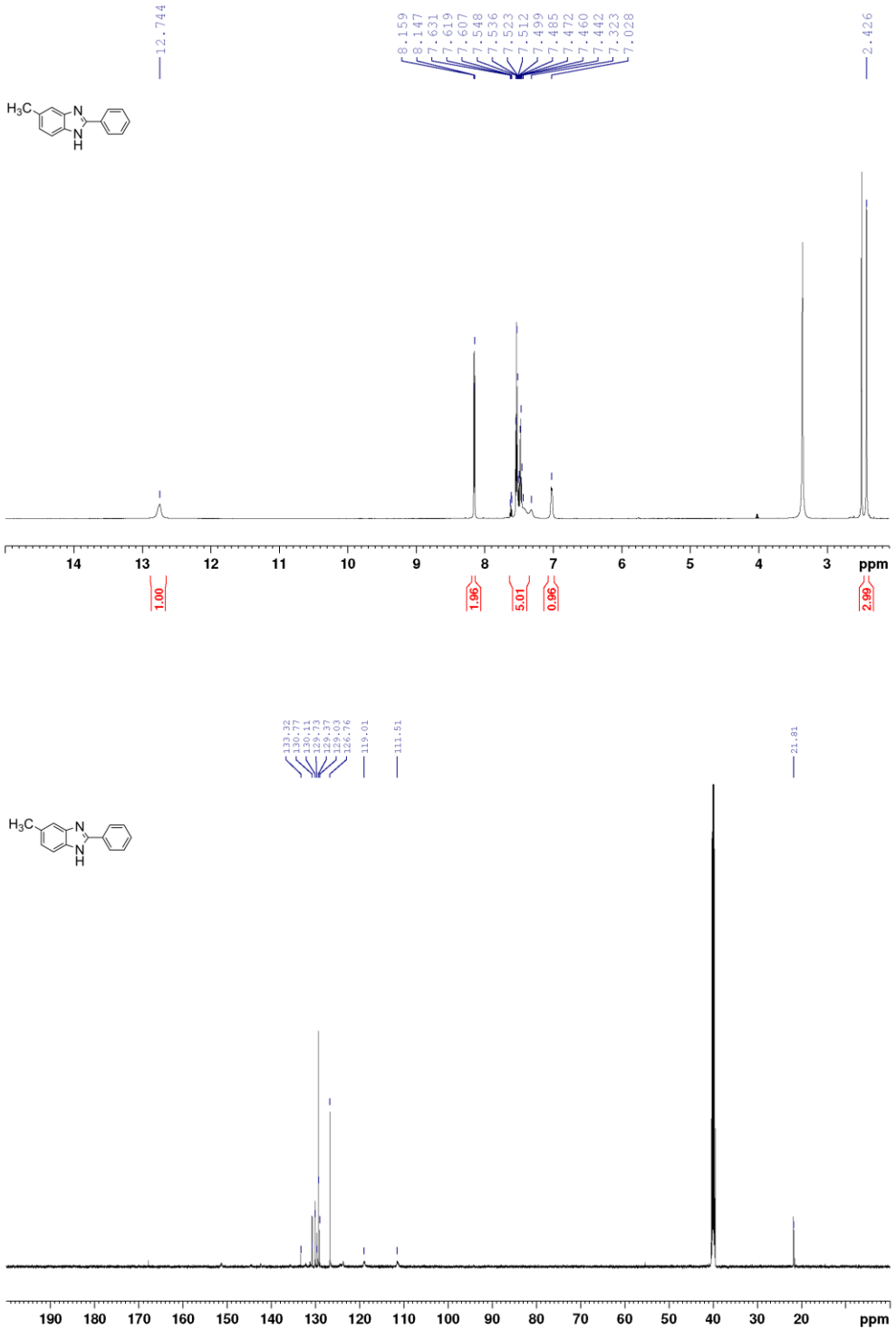

Supplementary Fig. 27 ^{1}H NMR and ^{13}C NMR spectra of **3e**.

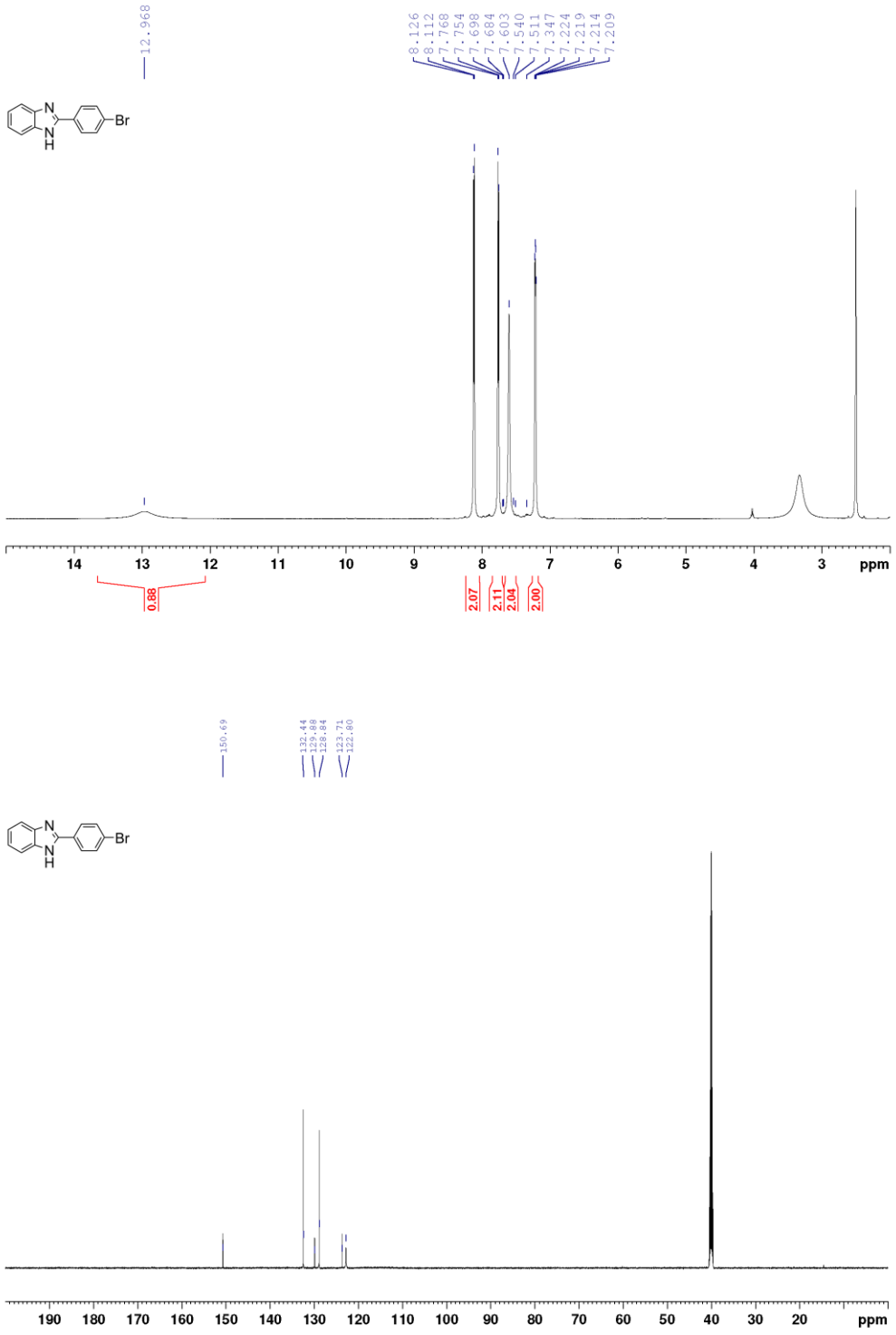

Supplementary Fig. 28 ^{1}H NMR and ^{13}C NMR spectra of **3f**.

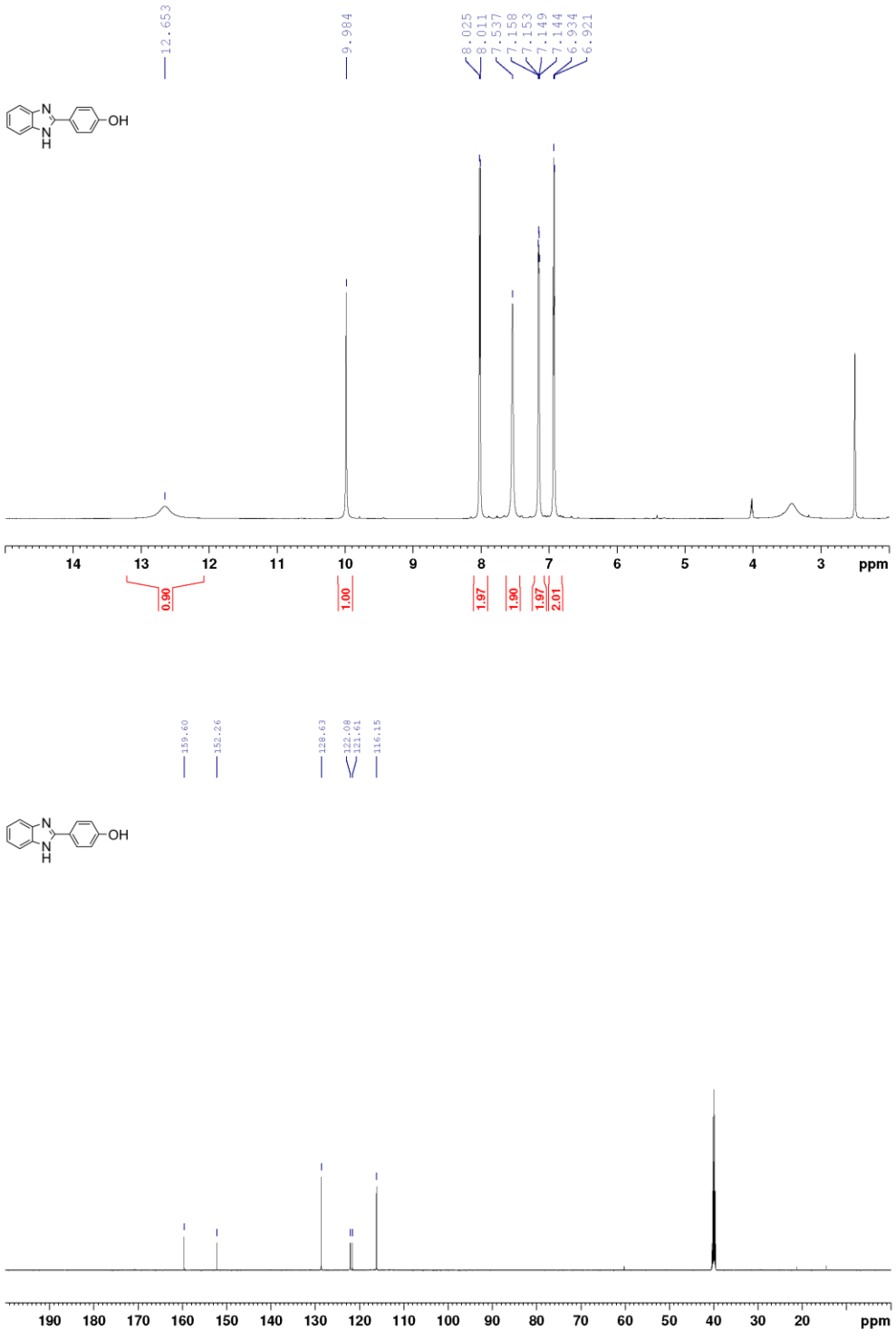

Supplementary Fig. 29 ^{1}H NMR and ^{13}C NMR spectra of **3g**.

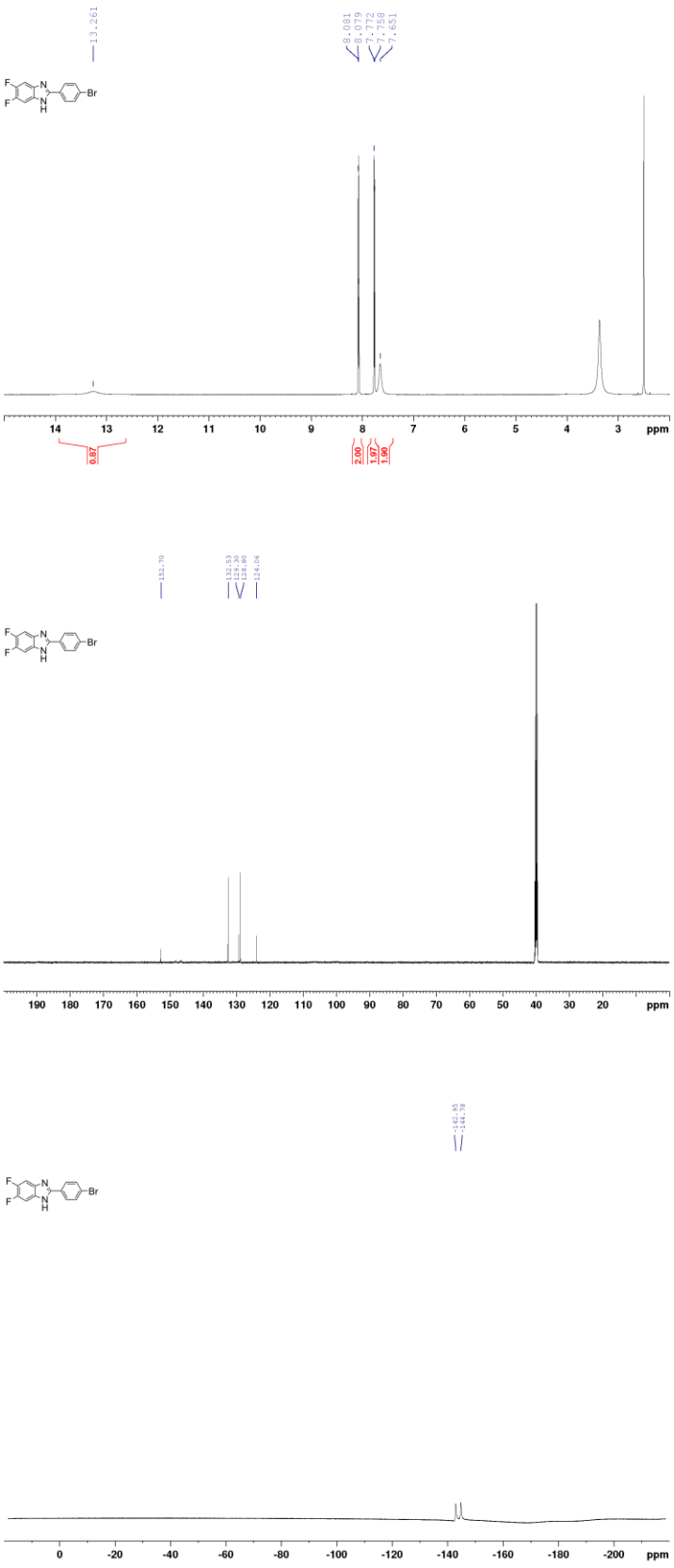

Supplementary Fig. 30 ^{1}H NMR, ^{13}C NMR, and ^{19}F NMR spectra of **3h**.

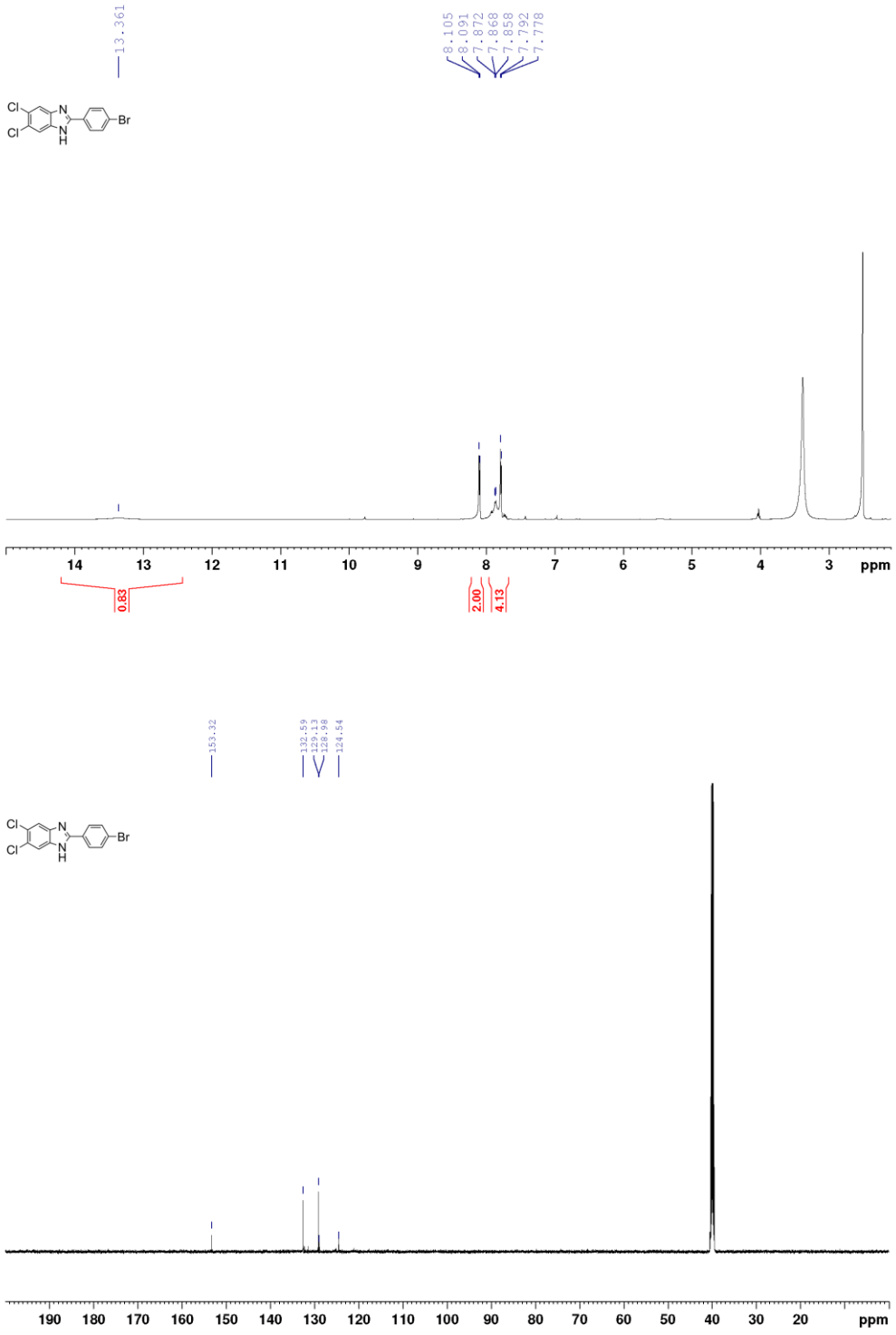

Supplementary Fig. 31 ^{1}H NMR and ^{13}C NMR spectra of **3i**.

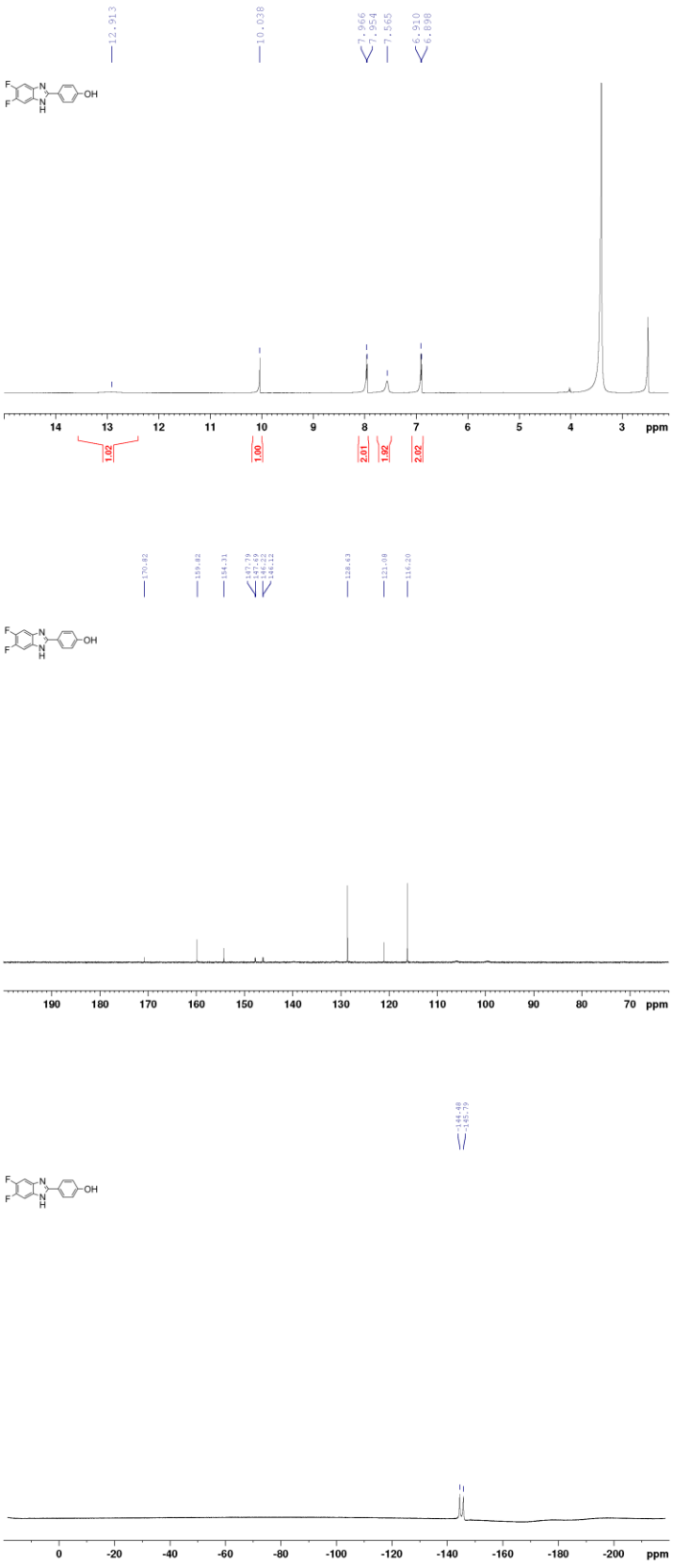

Supplementary Fig. 32 ^{1}H NMR, ^{13}C NMR, and ^{19}F NMR spectra of **3j**.

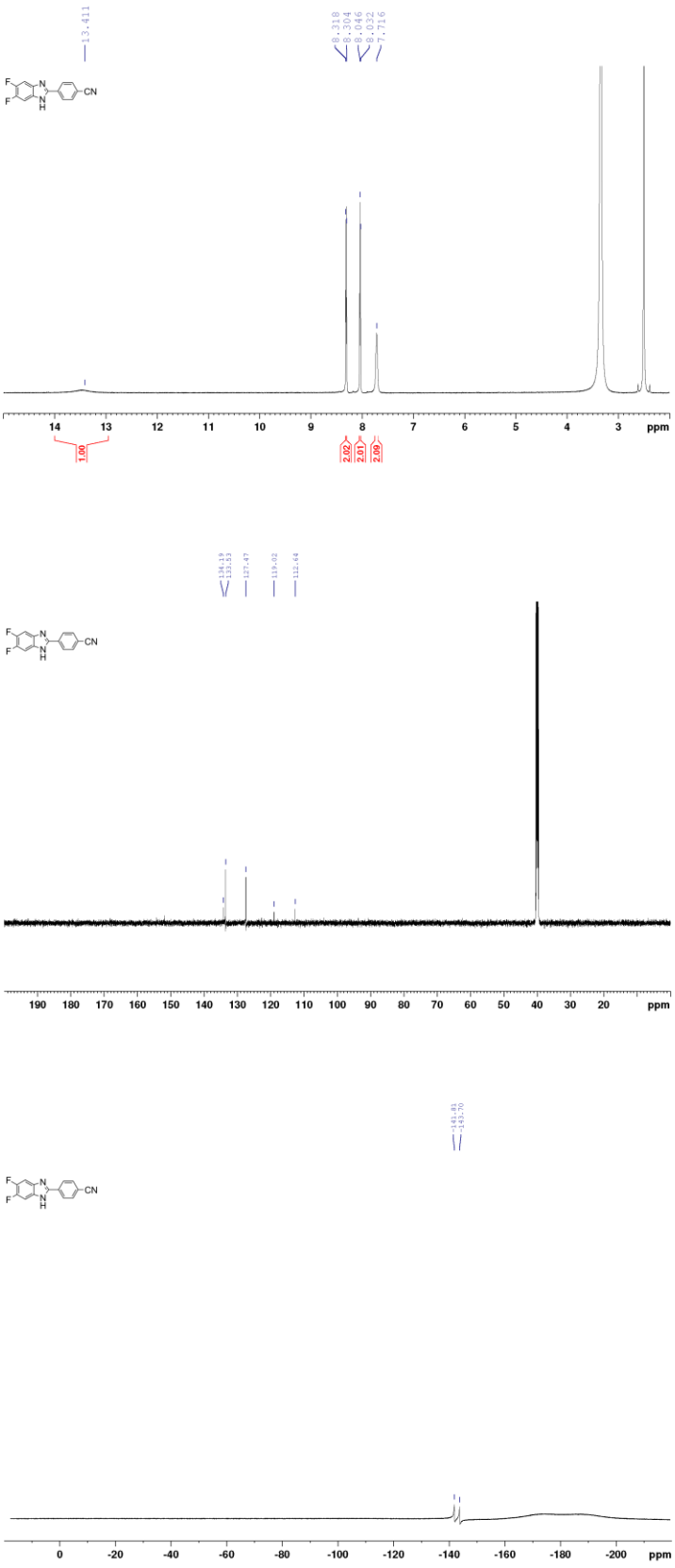

Supplementary Fig. 33 ^{1}H NMR, ^{13}C NMR, and ^{19}F NMR spectra of **3k**.

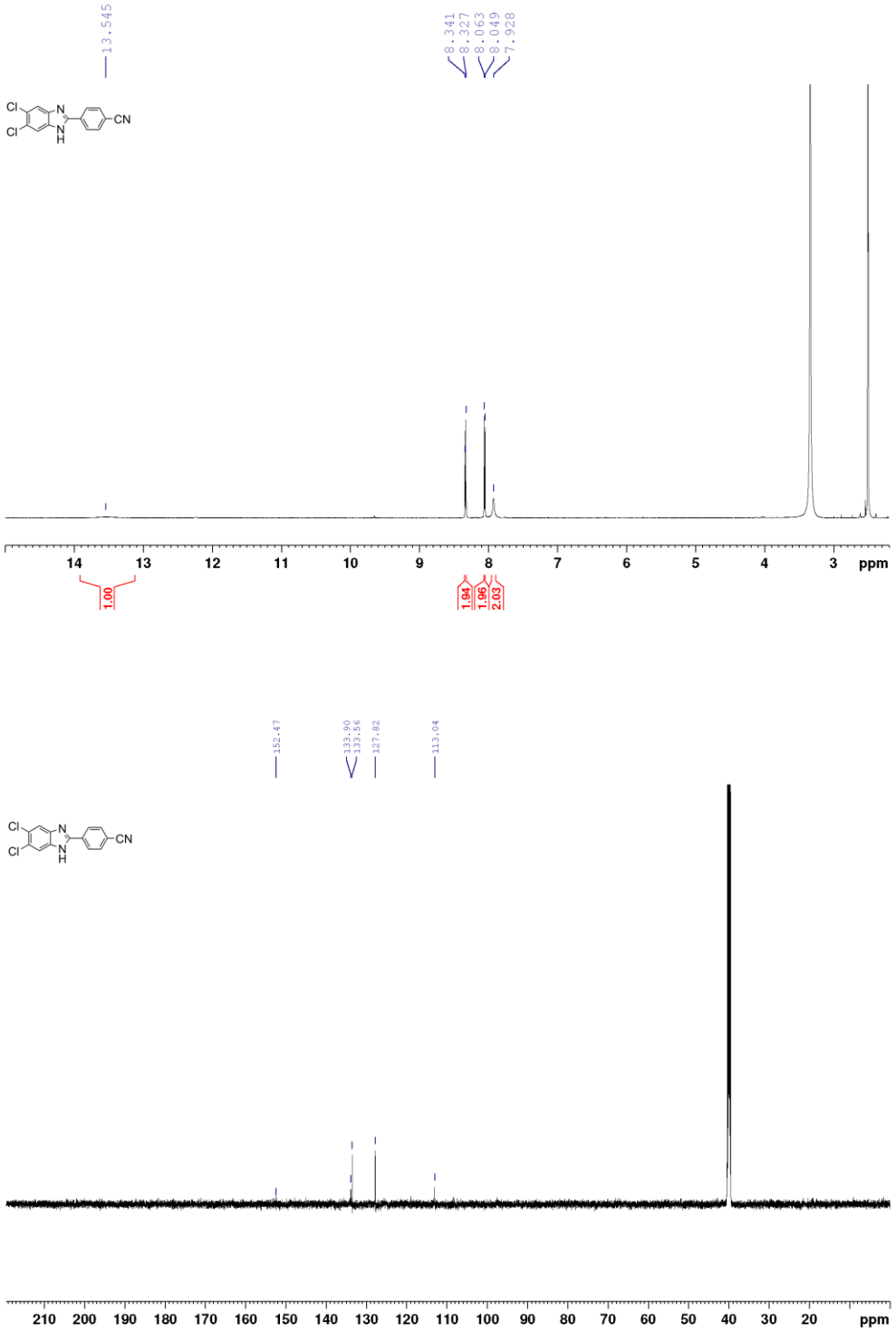

Supplementary Fig. 34 ^{1}H NMR and ^{13}C NMR spectra of **3l**.

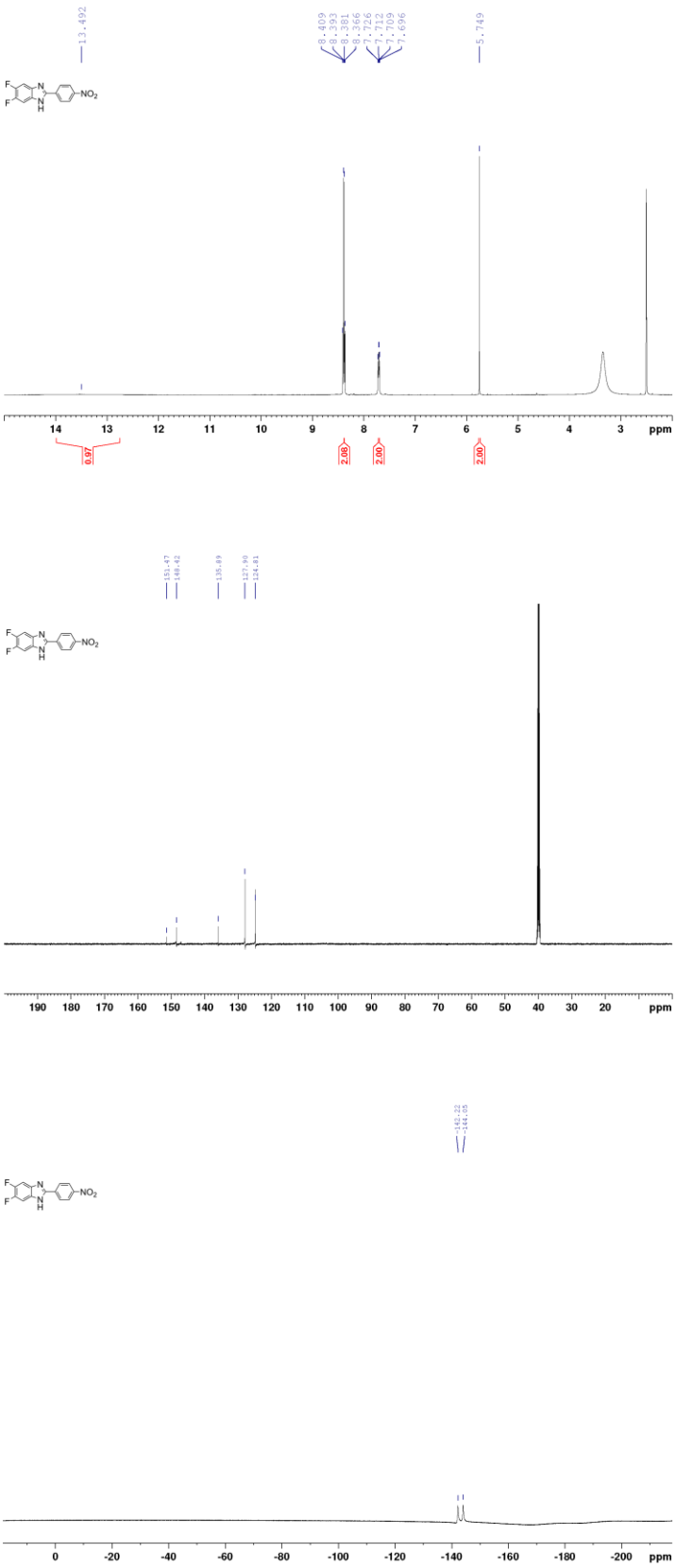

Supplementary Fig. 35 ^{1}H NMR, ^{13}C NMR, and ^{19}F NMR spectra of **3m**.

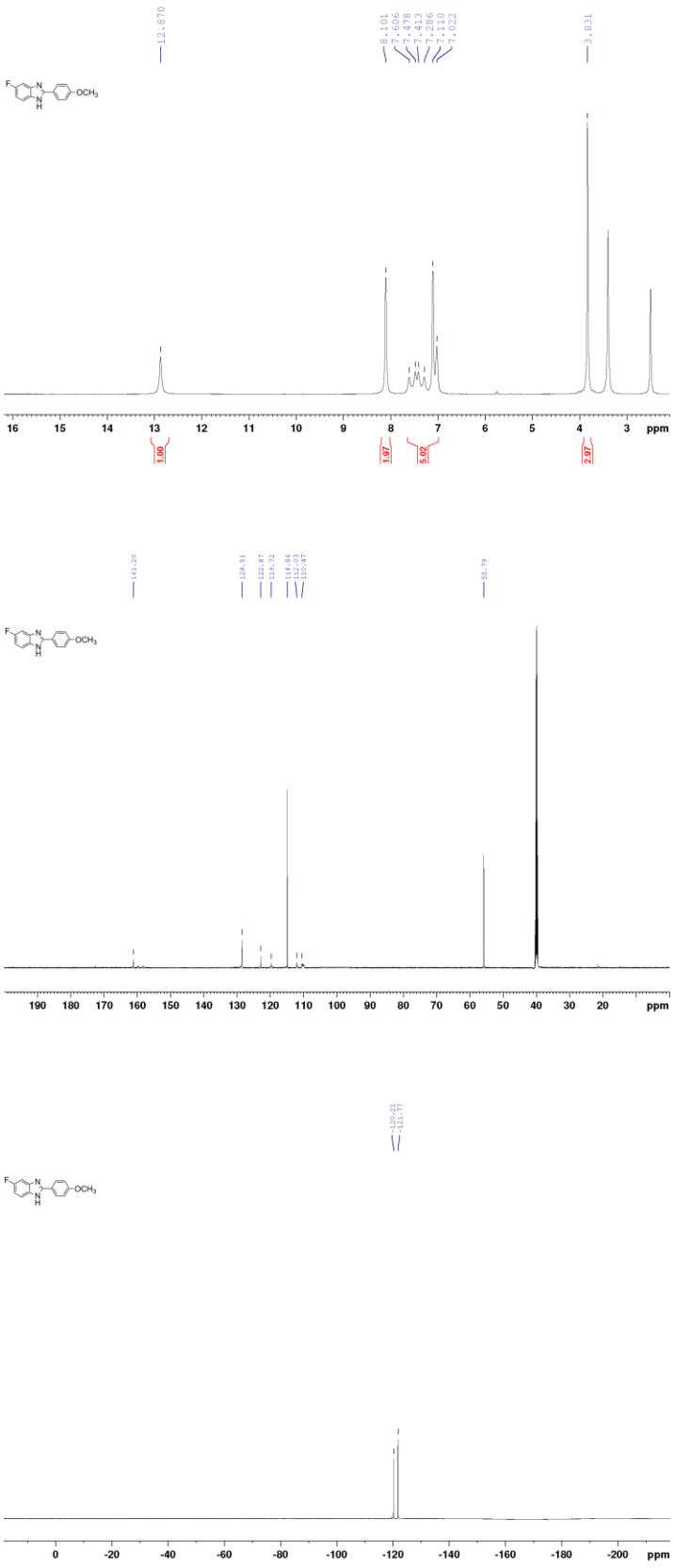

Supplementary Fig. 36 ^{1}H NMR, ^{13}C NMR, and ^{19}F NMR spectra of **3n**.

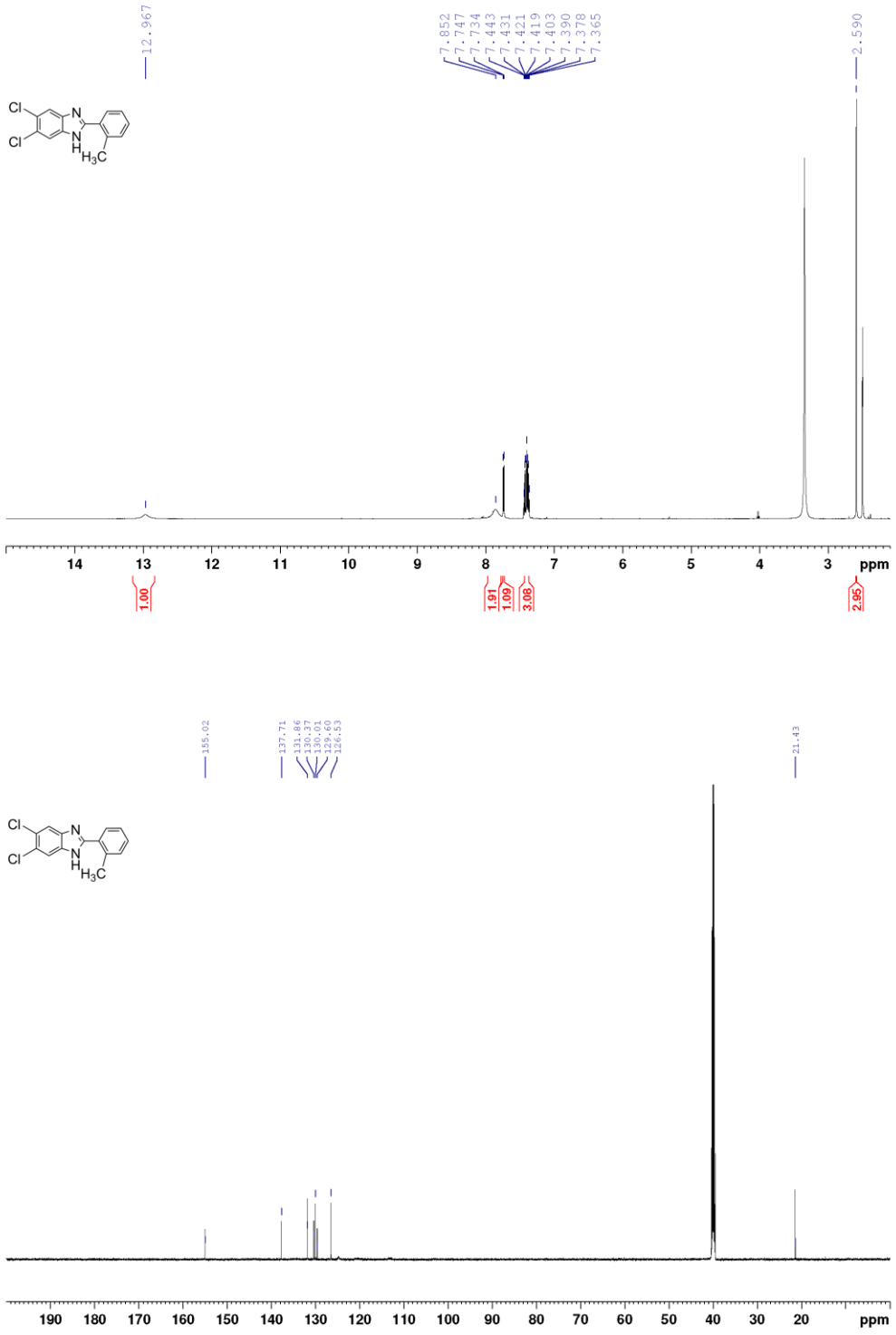

Supplementary Fig. 37 ^{1}H NMR and ^{13}C NMR spectra of **3o**.

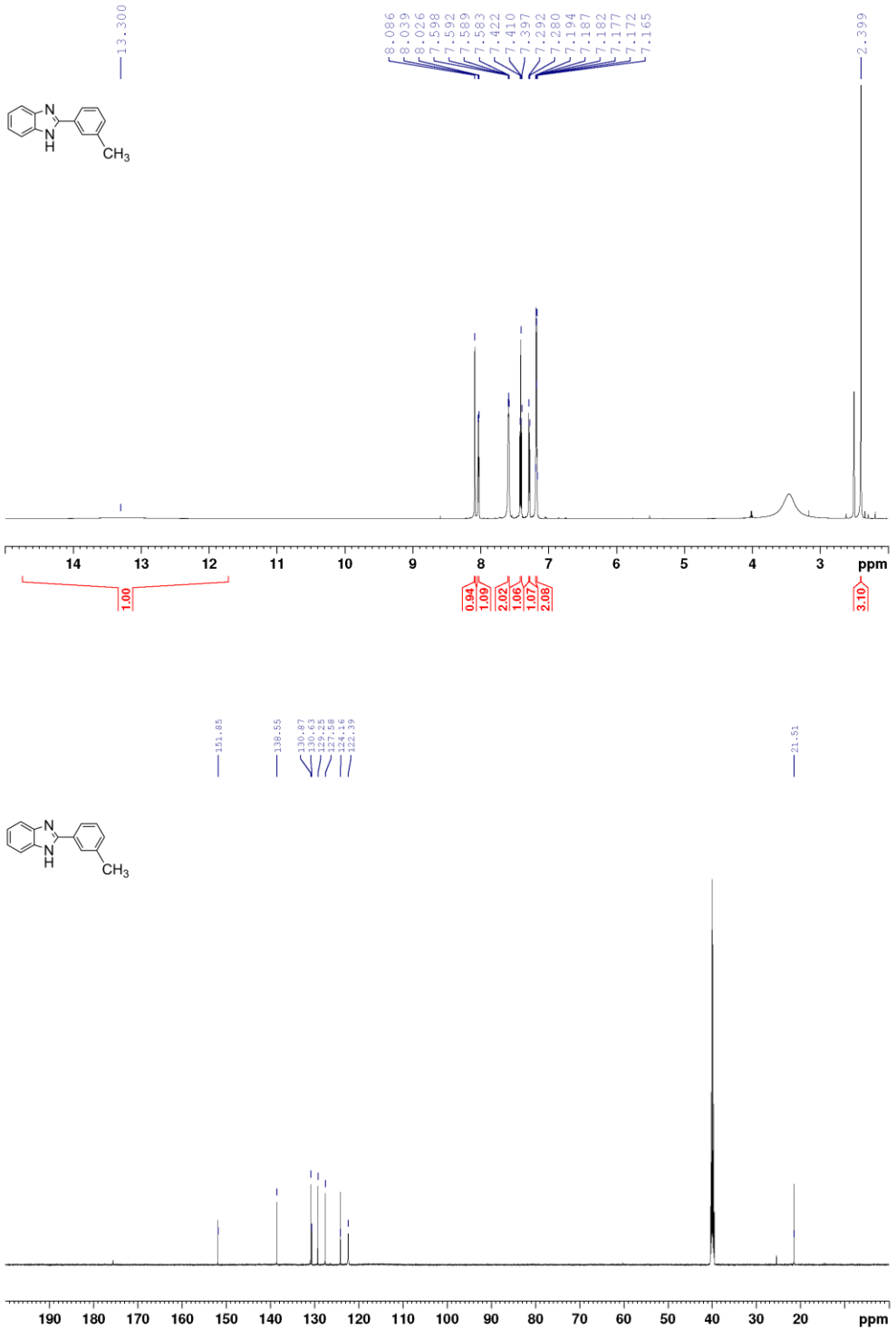

Supplementary Fig. 38 ^{1}H NMR and ^{13}C NMR spectra of **3p**.

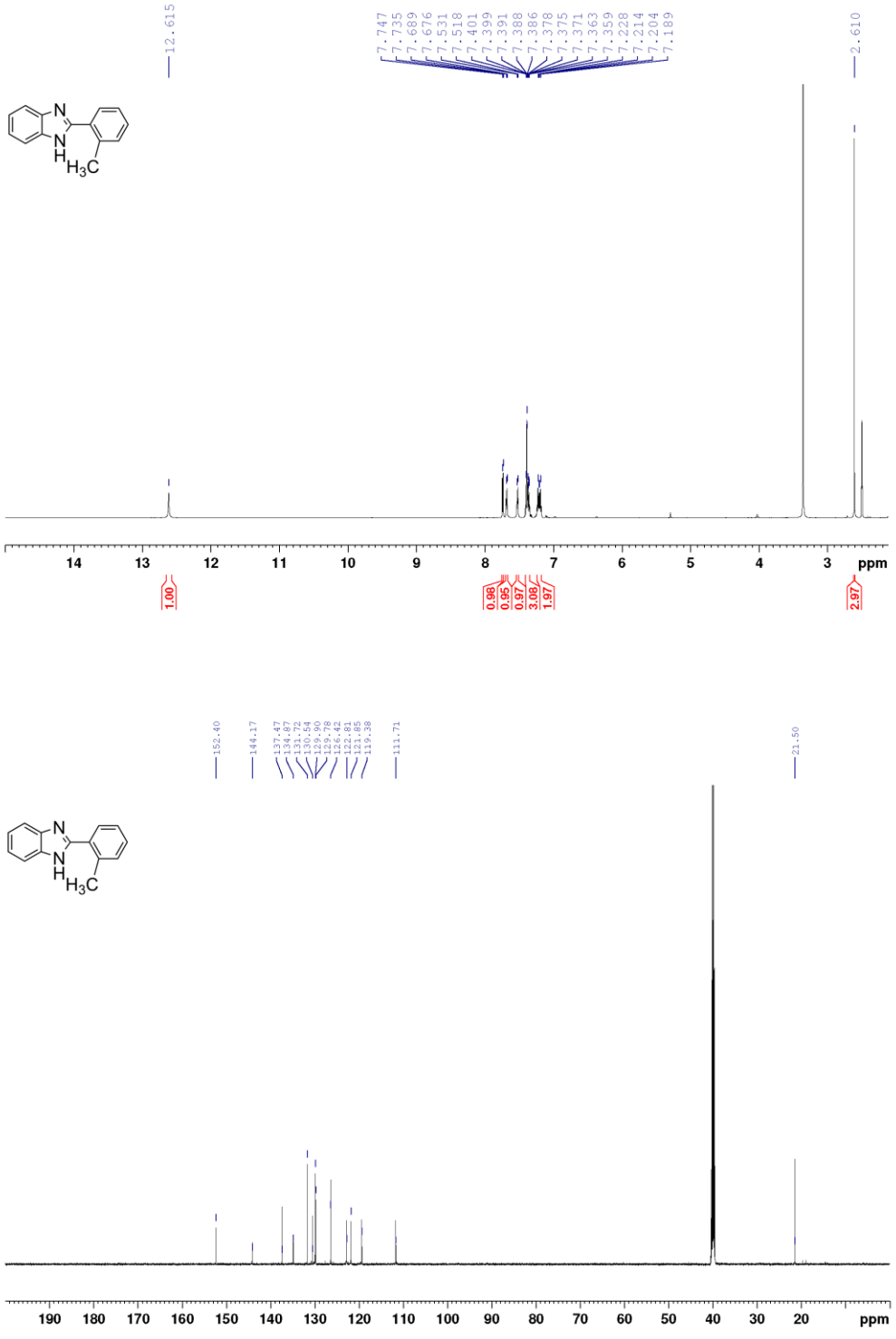

Supplementary Fig. 39 ^{1}H NMR and ^{13}C NMR spectra of **3q**.

9. References

[1] X. Zhao, H. Pang, D. Huang, G. Liu, J. Hu, Y. Xiang, *Angew. Chem. Int. Ed.* **2022**, e202208833.